AD-A081 897 AIR FORCE INST OF TECH WRIGHT-PATTERSON AFB OH SCHOO--ETC F/G 20/5
STUDY OF THE CORRELATION BETWEEN DEGRADATION OF KITON RED S LAS--ETC(U)
DEC 78 J M RABINS
UNCLASSIFIED AFIT/GEP/AA/78D-1 NL

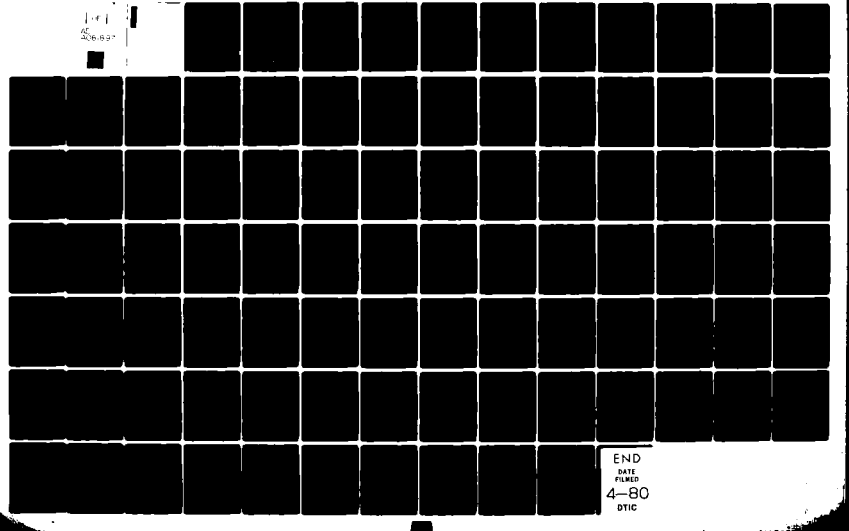

STUDY OF THE CORRELATION BETWEEN DEGRADATION OF KITON RED S LASER DYE AND DEGRADATION OF LASER ENERGY UNDER FLASH CONDITIONS

THESIS

AFIT/GEP/AA/78D-1

John M. Rabins
Capt USAF

Approved for public release; distribution unlimited

(14) AFIT/GEP/AA/78D-1

(6) STUDY OF THE CORRELATION BETWEEN DEGRADATION OF KITON RED S LASER DYE AND DEGRADATION OF LASER ENERGY UNDER FLASH CONDITIONS

(9) Master's ~~THESIS~~

Presented to the Faculty of the School of Engineering
of the Air Force Institute of Technology
Air University
in Partial Fulfillment of the
Requirements for the Degree of
Master of Science

(12) 92

(10) by
John M. Rabins, B.S.
Capt USAF
Graduate Engineering Physics

(11) Dec [redacted] 78

Approved for public release; distribution unlimited

Acknowledgements

This project was completed with the help of a lot of people. In particular, I am indebted to my advisor, Dr. Ernest Dorko, for his guidance, timely suggestions, and enthusiasm throughout the work. I would like to thank those at the Air Force Avionics Laboratory, Capt Sidney Johnson, Lt Gary Smith, Mr. Frank Kile, Mr. Sandy Smith, and Mr. Robert Wade, who gave freely of their time to help insure successful and meaningful results. I would also like to thank Mr. William Baker, Mr. H. Leroy Cannon, and Mr. Russell Murry for their help in building equipment and procuring necessary supplies. Finally, I would like to thank Mr. Mark Pippin for his help with the IR calibration curve and Capt Bruce Anderson for his help with the computations.

John M. Rabins

Contents

List of Figures

List of Tables

List of Symbols

Symbol	
A	Absorbance at peak
A_o	Absorbance at tie-line
a	Exponent
c	Concentration, mole/liter
D	Density of solvent, g/ml
d	Sample thickness, cm
I	Intensity, watt/cm^2
I_o	Incident intensity, watt/cm^2
K	Apparent rate constant, mole/liter-shot
K_H	Henry's law constant, mm Hg
k	Actual rate constant, mole/liter-shot
M_w	Molecular weight of solvent, g/g-mole
n	Reaction order
P_A	Partial pressure of gas A, mm Hg
R_1, R_2	Radicals
r	Correlation coefficient
r^2	Coefficient of determination
S	Number of flashlamp pulses
T	Transmittance at peak
T_o	Transmittance at tie-line
T_s	Temperature of solution, C
x_A	Mole fraction of A
α	Bunsen absorption coefficient
ϵ	Molar absorptivity (extinction coefficient), liter/mole-cm

Abstract

The laser dye Kiton Red S dissolved in ethanol was degraded under flashlamp excitation in a dye laser. Data obtained with infrared spectral analysis were used to construct plots of dye concentration versus shot number. From these plots the degradation reaction was found to be zeroth order in Kiton Red S. A rate equation was determined. Laser energy was monitored in order to allow for a comparison between laser degradation and dye degradation. The effect of both different oxygen concentrations and different excitation wavelengths on the reaction rate was observed. Based upon the experimental results a reaction mechanism was proposed. Two photoreaction products were postulated, one which absorbs laser radiation, and another which is reactive with the triplet dye molecules.

STUDY OF THE CORRELATION BETWEEN DEGRADATION OF KITON RED S LASER DYE AND DEGRADATION OF LASER ENERGY UNDER FLASH CONDITIONS

I. Introduction

Background

The use of an organic dye as a viable laser medium has been of interest since the advent of the laser. The first report of dye laser action was made in 1966 by Sorokin and Lankard (Ref 28:649) and since then dye lasers have been made to operate from the ultraviolet (UV) to the near infrared (IR) region of the electromagnetic spectrum. The quality which makes dyes so important in laser technology is the wide-range tunability afforded by the complex organic molecules. Dye lasers also offer moderate power or energy and excellent efficiency.

Affecting the utility of these lasers is the fact that all dyes photochemically dissociate with use, thereby causing various undesirable effects. These include a shift in the untuned peak spectral output, a decrease in laser output, an increased laser threshold, and a shift in the transverse laser beam mode. The factors causing this dye degradation are varied and still under investigation; they include the concentration of oxygen in solution and the excitation-source energy spectrum.

Kiton Red S (KRS), a dye of considerable interest to the Air Force, has been extensively investigated under continuous wave (CW) excitation (Ref 25) and partially investigated under flashlamp pumping (Ref 17). Two important conclusions were drawn from the CW experiments with regard to the degradation of KRS in ethanol. First, under CW excitation the

rate of photolytic degradation is not affected by the concentration of KRS. Also, the reaction rate is accelerated with greater oxygen concentration in solution (Ref 25:35). In addition, UV light below 250 nm has been found experimentally to cause the degradation associated with flashlamp excitation (Ref 17), and laser energy output has been shown to decrease dramatically with small changes in dye concentration due to degradation (Ref 17 and 25).

Research Objectives

The primary objective of this investigation was to study the causes of photolytic degradation of KRS in ethanol during lasing. Especially important in achieving this objective was the determination of the role of oxygen and excitation wavelength on the degradation reaction. IR, visible, and UV techniques were employed to provide insight into changes in the dye solution with time. This information, together with laser energy readings over time, was then used to help explain changes in the laser characteristics in terms of the dye solution degradation.

II. Theory

Dye Chemistry and Energy Schemes

Kiton Red S (the sodium salt of sulforhodamine B) is an efficient laser dye over the range 589 nm - 642 nm (Ref 32:348). This dye has demonstrated both long lasing lifetimes and efficiencies up to 1.4 percent in a coaxial flashlamp-pumped laser operated in a single-pulse mode (Ref 6:1). The polar solvent ethanol is often used since KRS is a polar molecule and because aggregation of organic dye molecules does not normally occur in organic solvents, even at very high concentrations (Ref 8:158-160).

KRS is representative of its family, the xanthenes, which includes the rhodamine dyes. The parent compound, xanthene, is pictured in Fig. 1, and the structure of KRS is shown in Fig. 2. This structure, which was

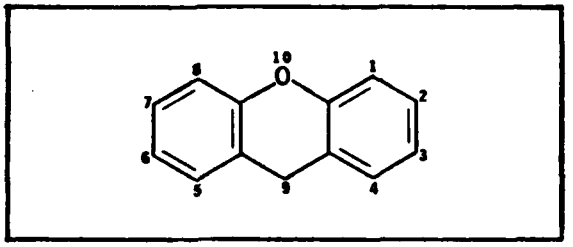

Fig. 1. The Parent Xanthene

determined using elemental analysis and nuclear magnetic resonance (Ref 7: 181), is strikingly similar to that of rhodamine B (Fig. 3). It has been found that the nature of the substituent bonded to the 9 carbon atom strongly influences the observed spectroscopy and lasing characteristics of these two xanthene dyes. Also, the chemistry of the 9 carbon atom has

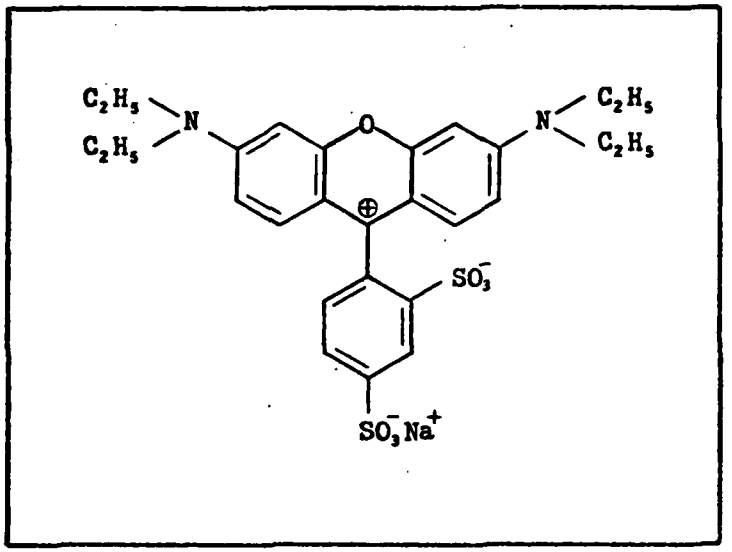

Fig. 2. Kiton Red S

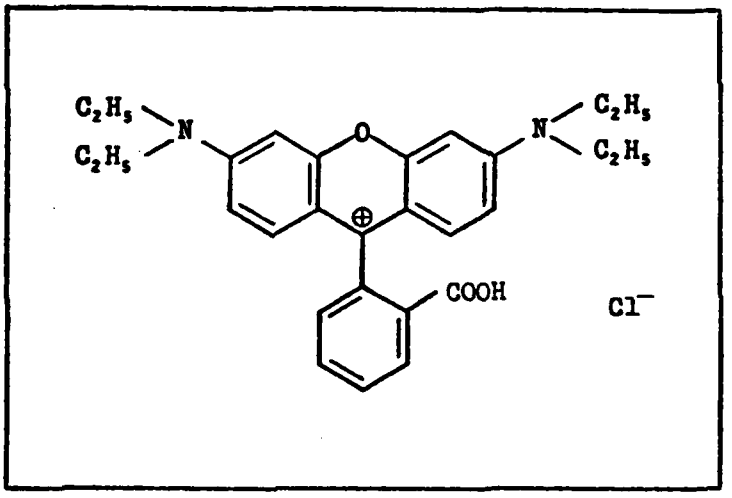

Fig. 3. Rhodamine B

been shown to affect the rate of intersystem crossing (singlet-to-triplet transitions) as well as the energy separation between the electronic states of the molecule (Ref 7:182).

KRS is seen to be symmetric. It has a π electron cloud extending

over the two nitrogen atoms, allowing the absorption transition $S_0 \rightarrow S_1$ to occur at relatively low energy (50.72 kcal/mole). This transition is a resonance excitation of an electron from the highest-filled bonding molecular orbital to the lowest antibonding molecular orbital ($\pi \rightarrow \pi^*$).

The energy levels of a typical organic dye are shown in Fig. 4.

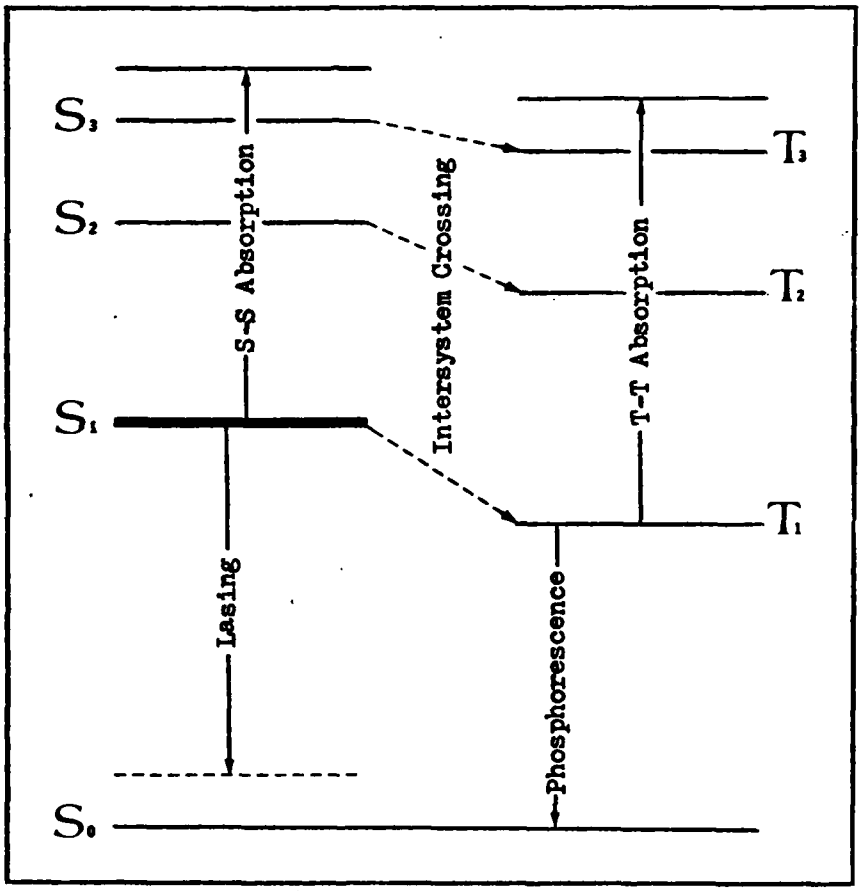

Fig. 4. Energy Level Diagram

Each electronic energy level is actually a band composed of a quasi-continuum of vibrational and rotational levels (Ref 28:649). The dye laser is a good example of the four-level system. Molecules are excited (during pumping) from the ground state to one of the higher excited

singlet states, from which they relax nonradiatively to the lowest vibronic level of S_1, the upper laser level. Under untuned lasing conditions, stimulated emission occurs from the bottom of S_1 to any of the unoccupied vibrational and rotational levels in the ground state S_0. From there they relax nonradiatively to the bottom of S_0. Organic dye molecules typically have a fluorescent decay time constant of between four and five nanoseconds, while the nonradiative relaxation time is on the order of picoseconds (Ref 24:35).

Ideally, for efficient lasing, the only method of deexciting the molecules in the S_1 energy level would be by stimulated emission. Realistically, however, there are several nonradiative processes that compete effectively with stimulated emission, thereby reducing the fluorescence efficiency in a manner that depends on the structure of the dye. These processes can be broken into two groups. First, there are those that cause a direct relaxation to the ground state S_0, also called internal conversion. Then there are those processes which allow a molecule in an excited singlet state to transition to the triplet manifold and relax to the lowest level T_1; these are illustrated in Fig. 4 and are referred to as intersystem crossing. Because of the relatively long lifetime of the triplet states (on the order of microseconds), the dye molecules commonly accumulate in the T_1 state during excitation. Besides robbing the system of valuable molecules which could be used for lasing, the intersystem crossing leads to triplet-triplet (T - T) absorption of both the laser light and the pump radiation. Intersystem crossing, then, acts as an effective energy sink within the cavity (Ref 8:145-152 and 19:411). For a detailed theoretical development of the effects of excited singlet state (S - S) absorption and T - T absorption

of pump and laser light, the reader is referred to the work of Teschke, Dienes, and Whinnery (Ref 30).

The accumulation of dye molecules in the triplet states can be reduced by adding what is commonly called a triplet quencher. The depopulation of these metastable triplet states by a chemical additive results from collisional transfer of energy from the triplet state of the dye to the chemical additive molecule. Triplet quenching occurs by collisions with the metastable state of indirect triplet quenchers, whereas for direct triplet quenchers it occurs by collisions with the more highly populated ground state (Ref 22:530). Many triplet quenchers have been added to dye laser systems with varying degrees of success. Some of the most effective are the direct quenchers, such as molecular oxygen, cyclooctatetraene (COT), and N-aminohomopiperidine. Oxygen has been shown to be an effective triplet quencher for members of the xanthene family (Ref 22:527). COT works well in quenching the triplet states of KRS and rhodamine 6G. Unlike oxygen, however, it quenches triplet states without increasing the rate at which excited singlet states are converted to triplet states via the intersystem crossing (Ref 31:85).

Dye Degradation

There are numerous reports dealing with the degradation mechanism of different lasing dyes. The degradation has been found to be permanent and primarily caused by the laser pump radiation (Ref 36:723). It has been found that the bleaching rate varies linearly with pump power (Ref 15:178) and inversely with solution volume (Ref 24:36). It is also known that this rate is strongly dependent upon the wavelength of the exciting radiation (Ref 3:308, 20, and 35:35). For KRS in solution, a cutoff filter which absorbed light below 290 nm was shown to extend the time required for complete bleaching by a factor of ten (Ref 27).

The Complexity of the Reaction. It is generally agreed that the degradation reaction mechanism for a dye under the influence of light is not simple. In fact, for KRS it is believed that extensive fragmentation occurs during degradation. Using a thin-layer chromatography (TLC) technique, Dorko et al were able to isolate from a degraded solution at least five different compounds with significantly different structures (Ref 6:4,13). In addition, the decline in laser output is not believed to be due to a simple loss of KRS molecules. Chemical analysis of degraded dye solution as well as fluorescence measurements have supported this finding, with a four percent decrease in fluorescence power corresponding to an 84 percent decrease in laser output energy (Ref 6:44-45 and 25:30). These preliminary findings suggest a multiplication factor ranging from 2 to a very large number.

There are reports of more than one reaction path occurring simultaneously in the degradation of various dyes (Ref 17, 18, and 36). It has also been suggested that the solvent is an integral part of the reaction mechanism. One group found that a chemical reaction between the triplet dye molecules of various rhodamines and their solvents (including ethanol) caused the photodegradation of the dye solution, and produced free radicals (Ref 37:94). Another investigation showed that the light from a mercury-argon discharge lamp affected the solvent methanol, and that the irradiated solvent accelerated the bleaching rate of rhodamine 6G (Ref 18:329). A striking result emerged from one other study (Ref 23:1126-1127), in which it was demonstrated that the preliminary irradiation of the solvent alone was practically equivalent to the irradiation of an ethanol solution of rhodamine 6G, in terms of reduced laser efficiency.

The photochemical reaction products also play a significant role in the degradation process. They are not normally laser-active, but they have been shown to absorb both laser and pump radiation (Ref 21, 23:1126, and 36:724). Further, the removal of reaction products has completely restored the laser activity of a previously-irradiated solution of rhodamine 6G in ethanol (Ref 23:1127). For rhodamine 6G in methanol, the products are believed to act catalytically on the degradation as the reaction progresses (Ref 18:328).

The Effect of Oxygen. Molecular oxygen has long been known to be an effective quencher of undesirable triplet states (Ref 8:158 and 26: 58). Unlike some other triplet quenchers, however, oxygen may also quench electronically-excited singlet-state molecules, and has also been known to increase the rate of intersystem crossing between the singlet- and triplet-state molecules (Ref 10:3 and 19:415). In addition, oxygen, upon photodissociation, can act as an oxidizing agent, and thus participate in the dye solution degradation reaction. Molecular oxygen photodissociates to atomic oxygen under the influence of UV light of wavelength below 240 nm (Ref 13:483).

The actual effects of oxygen in a degrading dye solution have been remarkably varied and seemingly contradictory. O'Brien demonstrated that oxygen accelerated the rate of degradation of KRS in ethanol when exposed to a mercury point source (Ref 25:35). Beer and Weber showed that oxygen increased the bleaching rate for rhodamine 6G in methanol (Ref 3:307-308). They irradiated the solution with a continuous argon laser. In another experiment with rhodamine 6G in methanol, Kato and Sugimura found that under exposure to far-UV light from a low-pressure mercury-argon lamp, the degradation was inhibited by oxygen (Ref 18:329-330). They suggested

that oxygen reacts preferentially with the methanol solvent, and that a second process leads to photobleaching once the oxygen has been consumed. Schwerzel has shown that oxygen slows the degradation rate of a KRS-methanol solution illuminated by a medium-pressure mercury arc lamp (Ref 27). Besides affecting the rate of dye degradation, oxygen has also been found to diminish the laser lifetime (Ref 17:64-65) and lead to the production of substances which absorb laser radiation (Ref 36:724).

There is some evidence that the triplet state is somehow responsible for photobleaching. Johnson demonstrated that the photodegradation rate for KRS in various solvents was slowed if the triplet quencher COT was added to the dye solution (Ref 17:73). Yamashita and Kashiwagi concluded, after directly detecting a decrease of T_1 molecules and an increase of free radicals during degradation, that a chemical reaction between the triplet dye molecules and the solvent led to photodegradation of various xanthene dyes in ethanol (Ref 37:94). Finally, from the results of Kato and Sugimura, Schwerzel has speculated that the photobleaching results by hydrogen abstraction from the solvent by the triplet state of rhodamine 6G, since the process does not begin until the triplet quencher (oxygen) has been consumed (Ref 27).

Absorption Spectrometry

The total energy of a molecule arises from translational, rotational, vibrational, and electronic energies. As a first approximation, these energies may be considered independently of one another. Electronic energy transitions typically result in absorption or emission in the UV and visible portions of the electromagnetic spectrum. Molecular vibrations produce absorption bands throughout most of the IR region of the spectrum. Rotational transitions give rise to absorption in the microwave or the far-IR

regions (Ref 4:1). Conversion between wavelength and transition energy is found in Table I.

Table I
Transition Energies at Various Wavelengths

Wavelength Range	Wavelength	Energy (kcal/mole)
X-rays	0.1 nm	2.86×10^{5}
	3 nm	9.54×10^{3}
Vacuum ultraviolet	200 nm	143
Ultraviolet	400 nm	72
Visible	800 nm	36
Very near infrared	3 μ	9.5
Near infrared	25 μ	1.1
Microwave	1 cm	2.86×10^{-3}

(Ref 5:198)

Absorption spectra can be useful in determining the energy structure, composition, quantity, and identity of a substance. Particularly useful in the identification of organic compounds is IR spectroscopy. Both quantitative and qualitative results may be obtained. Of special interest is the fundamental transition, that transition from the ground state to the vibrationally-excited state of lowest energy. This transition is normally located in the near-IR portion of the spectrum.

Most organic molecules contain a large number of bound carbon atoms whose bending and stretching motions couple in a complicated fashion.

The result is a very complex pattern of bands in the spectral region from 7μ to 13μ. Much of the pattern depends on the total molecular skeleton, and this part of the spectrum is commonly referred to as the fingerprint region, as it is unique to a particular molecule. Thus, while it is not normally possible to assign the individual bands in this pattern to different pairs or groups of atoms, the entire pattern is useful in the identification of a compound (Ref 2:31-33).

UV and visible spectra, generally recorded between 100 nm and 700 nm, are not necessarily unique for different compounds. Hence, for identification purposes, UV and visible spectroscopy does not offer the degree of specificity afforded by IR techniques. Also, the region below about 180 nm is difficult to observe experimentally since molecular oxygen absorbs in this region. Comparative measurements between the reference and sample windows of the spectrophotometer are therefore difficult to make, unless the air surrounding the samples is replaced by a non-absorbing gas. In spite of these limitations much has been learned, via UV and visible spectroscopy, of energy structure and bonding schemes for many compounds. Although these spectra have been of little use in the study of saturated organic molecules, they have provided valuable information with respect to unsaturated, and especially conjugated systems (Ref 2: 57-60).

If a parallel beam of monochromatic radiation is incident upon a slab of absorbing material of uniform thickness which is perpendicular to the beam, the intensity of radiation transmitted by the sample is given by the Beer-Lambert law:

$$I = I_o e^{-\epsilon c d} \qquad (1)$$

where I_0 is the intensity of the incident radiation, I is the intensity after passing through a sample of thickness d, and c is the concentration of the solution. ϵ, a constant characteristic of the substance under examination, is commonly called the molar absorptivity or molar extinction coefficient. Defining the transmittance T as I/I_0, Eq (1) can be transformed into

$$T = e^{-\epsilon cd} \tag{2}$$

The absorbance A is defined as

$$A = -\log T \tag{3}$$

Substituting Eq (2) into Eq (3) yields

$$A = \frac{\epsilon}{2.3} cd \tag{4}$$

For a sample of constant thickness, a plot of absorbance versus concentration should thus yield a straight line for the range of concentrations in which the Beer-Lambert law is valid (i.e. the region in which the solution is optically thin).

Reaction Kinetics

Rate Expression. It is usual to define the rate of a reaction as the rate of change of concentration for one of the reactants or products involved. The functional relation between rate and concentration, also called the rate expression, can be complicated, but is often written

$$\frac{d[A]}{dt} = -K[A]^a[B]^b[C]^c \cdots \tag{5}$$

where A, B, and C are reactants and K is the rate constant. Generally

it is not possible to predict the rate expression for a particular reaction simply by having knowledge of the stoichiometric equation. For rate expressions of the form of Eq (5) the order of the reaction, n, is defined as the sum of all the exponents of the concentrations, or

$$n = a + b + c + \ldots \tag{6}$$

Similarly, each individual exponent is called the order with respect to that particular component. For example, in Eq (5) b would be the order with respect to the component B, or simply the order in B. These individual orders not only point out how sensitive the system is to changes in the concentration of each species, but may also suggest the chemical mechanism of the reaction (Ref 29:8). The exponents are very often simple positive integers, but occasionally they may be fractional or even negative, depending upon the reaction's complexity.

If conditions for a particular reaction are such that the concentration of one or more of the reactants is constant or nearly constant during an experiment, these concentration factors may be included in the rate constant K. This occurs for catalytic reactions with the catalyst concentration remaining constant during the run, for cases where the concentration of one reactant overwhelmingly exceeds that of another, or for cases where efforts are taken to maintain a constant concentration of one or more of the reactants. When these conditions exist, the reaction is sometimes referred to as pseudo-nth order, where n is the sum of the exponents of those concentration factors which change during the run (Ref 12:10-11).

In the following development only those reactions which go to completion will be considered. Therefore, the reverse reaction rates are

assumed to be zero. For a reaction whose rate depends solely on the concentration of one reactant A

$$A + \text{other reactants} \longrightarrow \text{products}$$

the rate expression is

$$\frac{d[A]}{dS} = -K[A]^n \tag{7}$$

where S is normally a time term. In the present discussion S is taken to represent the number of flashlamp pulses. This equation may be readily integrated after separating variables. The limits of integration are $[A] = [A]_0$ at $S = 0$ and $[A] = [A]$ at any S.

$$\frac{d[A]}{[A]^n} = -K\,dS \tag{8}$$

$$\int_{[A]_0}^{[A]} \frac{d[A]}{[A]^n} = -K\int_0^S dS \tag{9}$$

The term zero order ($n = 0$) is applied to a reaction whose rate is completely independent of concentration, so that Eq (9) becomes

$$\int_{[A]_0}^{[A]} d[A] = -K\int_0^S dS \tag{10}$$

On integration

$$[A] = [A]_0 - KS \tag{11}$$

and a plot of [A] versus S yields a straight line with a slope equal to $-K$ and a y-intercept equal to $[A]_0$.

When $n = 1$ Eq (7) represents a first order rate expression. When

integrated it yields

$$\ln [A] = \ln [A]_0 - KS \tag{12}$$

or

$$[A] = [A]_0 \, e^{-KS} \tag{13}$$

A plot of ln [A] versus S produces a straight line whose slope is - K and whose intercept equals ln [A] .

When $n > 1$ the resulting nth order equation, when integrated, gives

$$\left[\frac{1}{n-1}\right]\left[\frac{1}{[A]^{n-1}} - \frac{1}{[A]_0^{n-1}}\right] = KS \tag{14}$$

and a plot of $\frac{1}{[A]^{n-1}}$ versus S is linear, with a slope of (n - 1) K and a y-intercept of $\frac{1}{[A]_0^{n-1}}$.

Henry's Law. The amount of a slightly soluble gas that dissolves in a liquid is, in the limit of zero concentration, directly proportional to the partial pressure of that gas above the solution, according to Henry's law (Ref 34:F.83). In equation form Henry's law appears as

$$K_H = \frac{P_A}{x_A} \tag{15}$$

where K_H is Henry's law constant, P_A is the partial pressure of the gas A, and x_A is the mole fraction of A dissolved in the solution (Ref 1:345).

III. Apparatus

The laser system used in the present study was a Phase-R DL 1100 flashlamp-pumped dye laser with a triaxial cavity configuration. A triaxial laser differs from a coaxial, or biaxial, laser (Fig. 5) by

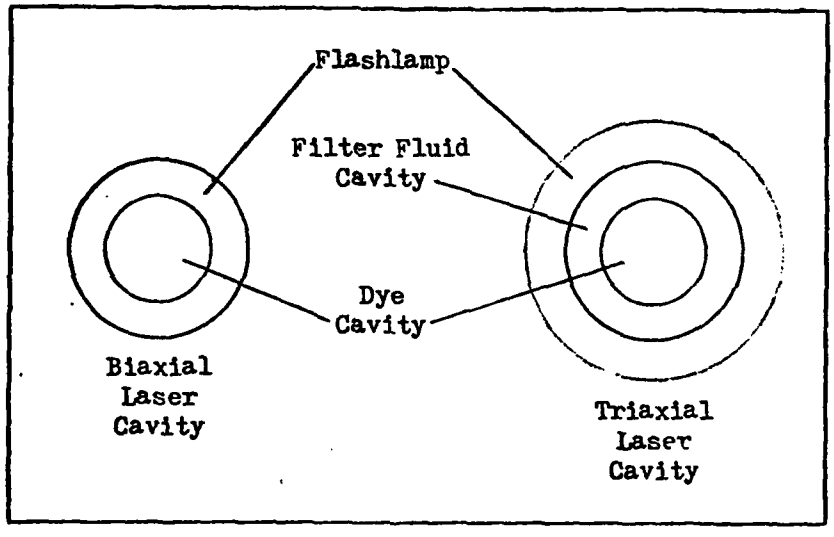

Fig. 5. Cross Section of Laser Cavities

the addition of an annular space between the dye and the flashlamp, through which a coolant typically flows. This annular region can be effectively used to filter the flashlamp radiation by the insertion of a filter fluid.

The laser system consisted of five parts: the laser head, the power supply and controls, the dye solution circuit, the filter fluid circuit, and the cooling circuit. These are shown schematically in Fig. 6. The laser head consisted of the DL 10 xenon flashlamp with a triaxial adaptor.

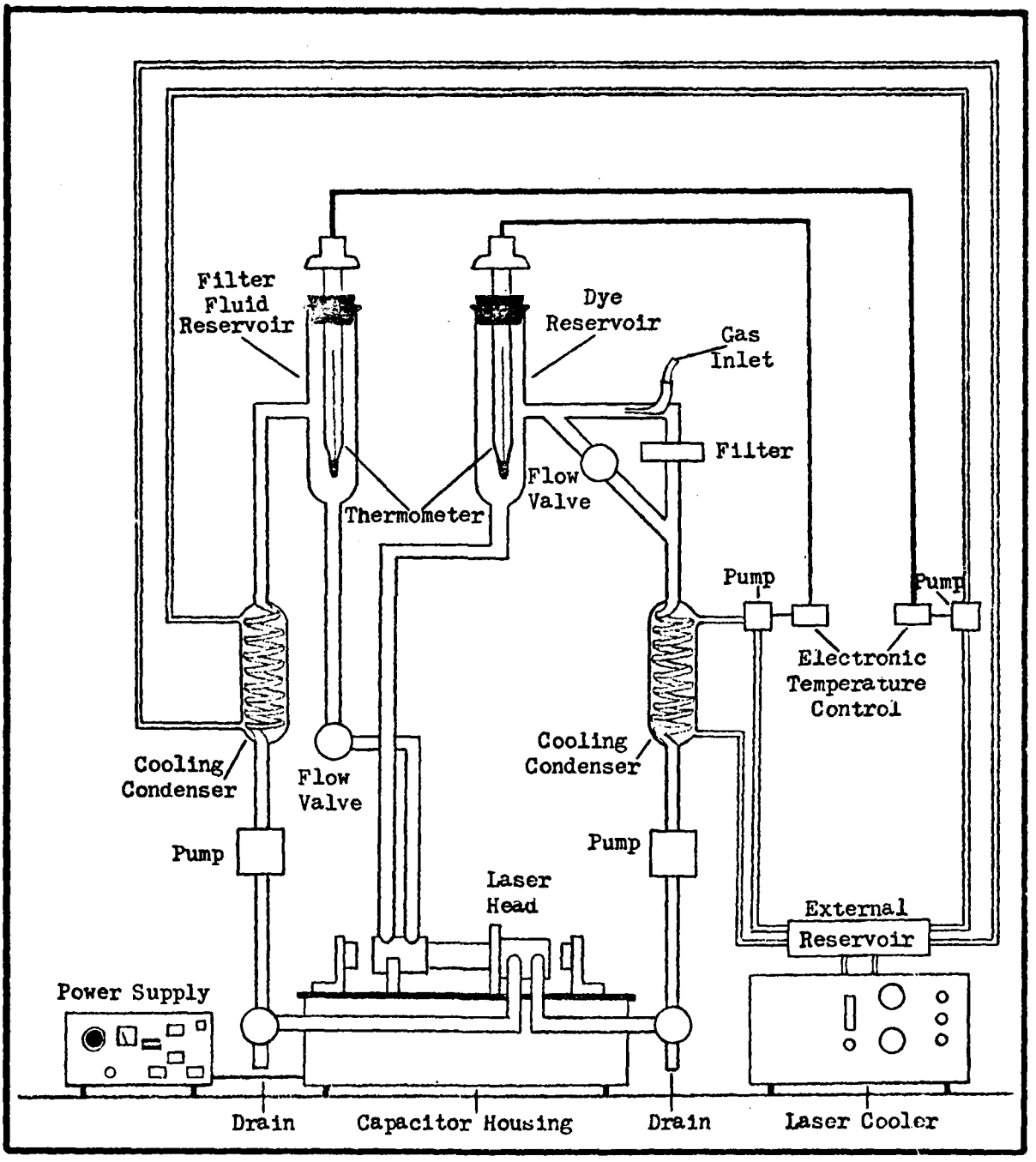

Fig. 6. Schematic of Dye Laser System

The flashlamp was annular in shape with an inner diameter of 10 mm and a length of 140 mm. The flashlamp produced a spectrum comparable to a 25,000 degree blackbody, and an average pulse was on the order of 500 nsec. The cylindrical dye cavity had a 6 mm inner diameter and an 8 mm outer diameter, and extended between two end windows which were 250 mm apart. The annular sleeve around the dye cavity (the filter fluid cavity) was 1 mm thick and extended along the entire length of the dye cavity. The laser head was flanked by flat mirrors which were separated by 280 mm and which had reflectivities of 22 percent and 99 percent. The power supply and controls were standard DL 1100 equipment.

The dye solution was circulated through the cavity by means of a March AC-3C-MD high-purity pump. Emerging from the laser head, the dye was pumped through a 15-inch cooling condenser, through a filter, and into the dye reservoir. From there the dye flowed back down to the laser head and through the laser cavity. The filter, a Millipore (Type LS) 5μ Teflon filter, had two functions. First, it helped trap and remove small foreign particles from the flowing dye solution. Second, it created a pressure head which forced cavitated bubbles back into solution. The dye solution circuit was constructed of glass and polypropylene tubing, with Teflon fittings.

The filter fluid was circulated through the annular space surrounding the dye cavity by means of a March MDX-MT-3 high-purity pump. From the laser head the filter fluid was pumped through a 15-inch cooling condenser into a reservoir, from where it flowed back to the laser head via a flow control valve. The filter fluid circuit was constructed of glass and Teflon tubing, with Teflon fittings.

The cooling circuit was designed control independently the tem-

peratures of the dye and filter fluid. It was necessary that the temperatures of the two circulating fluids remain equal to each other in order to avoid radial thermal gradients in the laser cavity which could severely degrade beam quality and output energy (Ref 10:21). The coolant, deionized water, flowed in a closed loop between a Korad KWC-5 laser cooler and a cooling coil which rested in an external reservoir of deionized water. The external reservoir was thereby maintained at a constant temperature. Two independent subcooling systems drew from the external reservoir. One subsystem pumped coolant through the dye cooling condenser, and the other through the filter fluid cooling condenser. Each subsystem utilized a Micro-Pump 7004-92 variable-speed gear pump which was connected to a Versa Therm 2149 electronic temperature control relay. The thermostat in each of the dye and filter fluid reservoirs was a temperature sensor with a 0.01 degree control accuracy.

In each experiment a selected gas (called the cover gas) was bubbled into the dye solution. The cover gas was fed into the circulating dye through a capillary inserted just above the dye filter. Bubbling was controlled with a needle valve on the gas mixture bottle.

The dye used throughout the experiments was Kiton Red S (purchased as Kiton Red 620 from the Exciton Company, Dayton, Ohio). It was dissolved in absolute dehydrated, reagent-grade ethyl alcohol. Laser beam energy measurements were made with a Quantronix 504 energy-power meter with an attached 501 energy receiver.

IV. Experimental Procedure

The general procedure is described first, followed by modifications and experimental details.

Flash Photolysis

Dye solution for the experiments was prepared in the following manner. A 304.5 mg sample of powdered KRS (580 g/g-mole) was weighed on an analytical balance. This material was then dissolved in 500 ml of ethanol, and the resulting solution was filtered through a Millipore (Type FG) 0.20μ Teflon filter to produce a 10^{-3} M solution. This filtration was necessary to remove salts and other impurities which were present in the powdered dye. Further dilution provided a 2×10^{-4} M solution for use in the experimental trials. This concentration provided efficient lasing and well-defined absorption peaks for the spectrophotometric analysis.

The dye reservoir was filled with 500 ml of 2×10^{-4} M KRS in ethanol and the filter fluid reservoir was filled with 500 ml of the appropriate filter fluid. The dye and filter fluid circulating pumps were then turned on, as well as the laser cooler, the coolant pumps, and the electronic temperature control relays. The discharge water temperature of the cooler was set at 15 C, and each of the dye and filter fluid thermostats was adjusted to 20 C. The cover gas was introduced to the circulating dye solution and allowed to bubble for two hours prior to lasing in order to permit equilibration of dissolved gas in the dye solution. It is possible, though, that a greater amount of time would be necessary for

complete equilibration. The laser was aligned in accordance with the manufacturer's instructions.

Just prior to lasing, a 2 ml sample of the dye was withdrawn with a syringe and stored for analysis. After lasing commenced, initial beam energy was determined over the first few shots. Samples of dye solution were withdrawn after 100 shots and 250 shots, and then after each 250-shot interval to 1000 shots, each 500-shot interval to 3000 shots, and each 1000-shot interval through 5000 shots. Energy readings were taken each time a sample was withdrawn, as well as at 1250 and 1750 shots. An energy value was determined by taking readings over four or five consecutive shots, and averaging the two most consistent values. The voltage across the capacitor bank immediately before pulsing the laser was 18 kilovolts, and the repetition rate was approximately 40 shots per minute.

Sample Analysis

Two sets of analyses were accomplished for each sample withdrawn during a flash photolysis trial.

IR Analysis. Fifteen hundredths gm of oven-dried potassium bromide (KBr) was placed into a stainless steel capsule along with 1 cc of dye solution which was withdrawn during the flash photolysis trial. KBr is transparent to IR radiation over the range 2μ - 15μ, and is thus a suitable substrate for the dye. The capsule was placed into a 5 ml beaker for support, and the capsule and beaker were then placed into an evaporation chamber. The evaporation chamber was a 500 ml side-arm flask immersed in a water bath which was maintained at 30 C. The chamber was evacuated by means of an attached aspirator assembly. After the ethanol solvent was completely evaporated, air was reintroduced into the

chamber and the capsule was removed. A steel ball bearing was placed into the capsule which was then capped and shaken for one minute on an amalgam shaker. One tenth gm of the resultant powder was placed into a desiccator to further dry for at least two hours. Then the powder was carefully transferred to a pellet die. The die was assembled and evacuated with a vacuum pump. With a hydraulic press, pressure of 20,000 psi was applied to the die for two minutes to produce a transparent pellet. The pellet was inserted into a holder which was attached to the sample window of a Perkin Elmer sodium chloride spectrophotometer, and a spectrum was obtained over a 15-minute scan time with the slit control on N. The baseline of the spectrum was adjusted to fall at 95 percent transmittance. Each spectrum was recorded on paper ruled for absorbance measurements, with the baseline near the top of the sheet and absorption peaks in the downward direction.

UV and Visible Analysis. The UV and visible analysis was performed with a Cary 14 recording spectrophotometer with a Universal percent transmittance slidewire, and two matched SCC quartz spectrophotometer cells of 1 mm path length each. The wavelength cutoff of the cells was below 180 nm.

The spectrophotometer was calibrated from 200 nm to 700 nm by establishing a baseline at 100 percent transmittance with ethanol in both the sample and reference cells. The baseline was deemed adequate if it did not deviate by more than one percent over this wavelength range. The sample cell was then filled with dye and a spectrum was obtained at a scan speed of 1 nm per second and a paper speed of $\frac{1}{2}$ inch per minute. The scan direction was always toward shorter wavelength, and the source was switched from visible to UV at 400 nm.

Experimental Details

Three calibration curves of absorption intensity versus dye concentration were prepared using a series of solutions with known concentrations from 2 $x10^{-5}$ M to 2 $x10^{-4}$ M. A curve was made for each of the IR, visible, and UV regions of interest by analyzing the solutions in the same manner as previously described. These curves (found in Appendix A) were later used to determine the concentration of KRS remaining in the samples withdrawn during the flash photolysis trials. For each of these calibration curves a least squares calculation of the data points was performed. Correlation coefficients of 0.99 for the IR calibration curve and of 1.00 for the visible and UV calibration curves indicate that the Beer-Lambert law is valid over the concentration values of interest.

Six experimental photolysis trials were accomplished in all. The first three were designed to determine the effect of oxygen on both dye and laser energy degradation. Each of these trials incorporated deionized water as a filter fluid. In the first trial, pure argon was bubbled into the dye solution in order to displace as much dissolved oxygen as possible. The second trial was performed with 10.3 percent oxygen in argon as a cover gas. The third trial was performed with dehumidified air (21 percent oxygen).

The final three trials were designed to elucidate the wavelength dependence of the dye and laser energy degradation. The first two of these trials (designated 4 and 5) were accomplished with ethanol as a filter fluid. The ethanol used was of the same make and grade as that used for the dye solvent. In the fourth trial argon was bubbled through the dye solution, and in the fifth trial dehumidified air was used as the cover gas. The final photolysis trial (designated 6) was done with an ethyl acetate filter fluid and dehumidified air as a cover gas.

Each experimental trial was carried through 5000 flashlamp pulses, with the exception of the fourth and sixth trials, which were carried through 3000 and 4000 pulses, respectively. In these two abbreviated trials, the results were extrapolated to 5000 shots for comparison purposes.

UV spectra were obtained for each of the three filter fluids used in the trials in order to determine the wavelength cutoff of each. The wavelength cutoff for a particular filter fluid is defined as that wavelength below which the transmittance is less than five percent. Also, in an attempt to see the effect (if any) of light on the solvent ethanol, a UV spectrum was made of the ethanol filter fluid of trial 5 after 5000 flashlamp pulses.

V. Data Reduction

The spectral data for each of the flash photolysis trials consisted of an IR spectrum and a UV-visible spectrum for each of the aliquots withdrawn during the trial. After the appropriate peaks were selected for measurement (one for each of the IR, visible, and UV ranges), the data for each sample was reduced by first measuring the size of each peak and then determining the concentration of KRS in solution by using the corresponding calibration curve. These data points were then plotted versus shot number and a least squares calculation of the data points was performed. In this way, three plots of concentration versus shot number were produced for each photolysis trial, one each for the IR, visible, and UV ranges.

The peak which was chosen for IR analysis was the strong peak at 7.5μ (see Fig. 7). O'Brien observed that the size of this peak is representative of the concentration of KRS in solution and that the disappearance of this peak indicates the depletion of KRS. He also noted that there was no interference with this peak by the spectrum of reaction products (Ref 25:21).

A UV-visible spectrum of undegraded KRS in ethanol is shown in Fig. 8. It can be seen that only one peak is available for analysis in the visible (the large peak at 552 nm) while there are two possible candidates in the UV (at 350 nm and at 255 nm). As it was difficult to consistently draw a stable tie-line over the peak at 255 nm, the 350 nm peak was selected to represent KRS concentration in this range. It is questionable whether either of the UV or visible peaks adequately represents the concentration

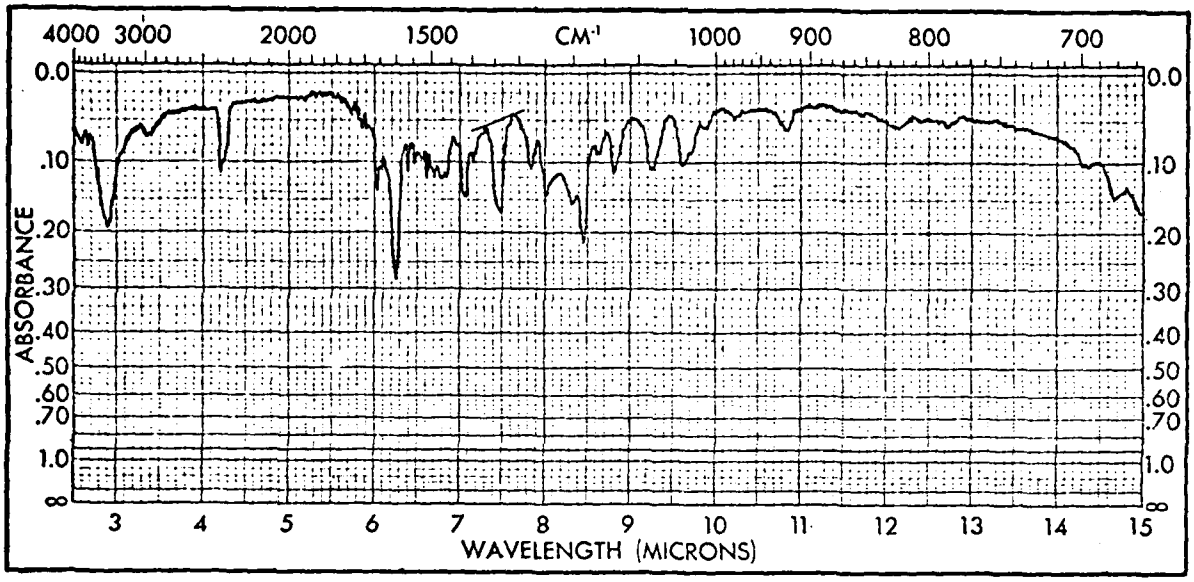

Fig. 7. IR Spectrum of Kiton Red S

of KRS alone, and henceforth concentration values obtained from either of these two peaks will be referred to as apparent concentrations. This point will be further explored in the next section.

All IR spectra were obtained on absorbance-ruled paper, which produces a plot of absorbance (as defined by Eq 3) versus wavelength, and so the size of the 7.5μ peak was determined by simply subtracting the absorbance A_0 at the tie-line from the absorbance A at the bottom of the peak. As the UV-visible spectra were obtained on transmittance-ruled paper, which produces a plot of transmittance (as defined by Eq 2) versus wavelength, the transmittance values were converted to absorbance values before subsequent manipulations were accomplished. The $(A - A_0)$ value was converted to a concentration value by referring to the appropriate calibration curve (Ref 11:182-195). This data reduction method is illustrated by a sample calculation which is given in Appendix B.

For each trial the beam energy was plotted against shot number and

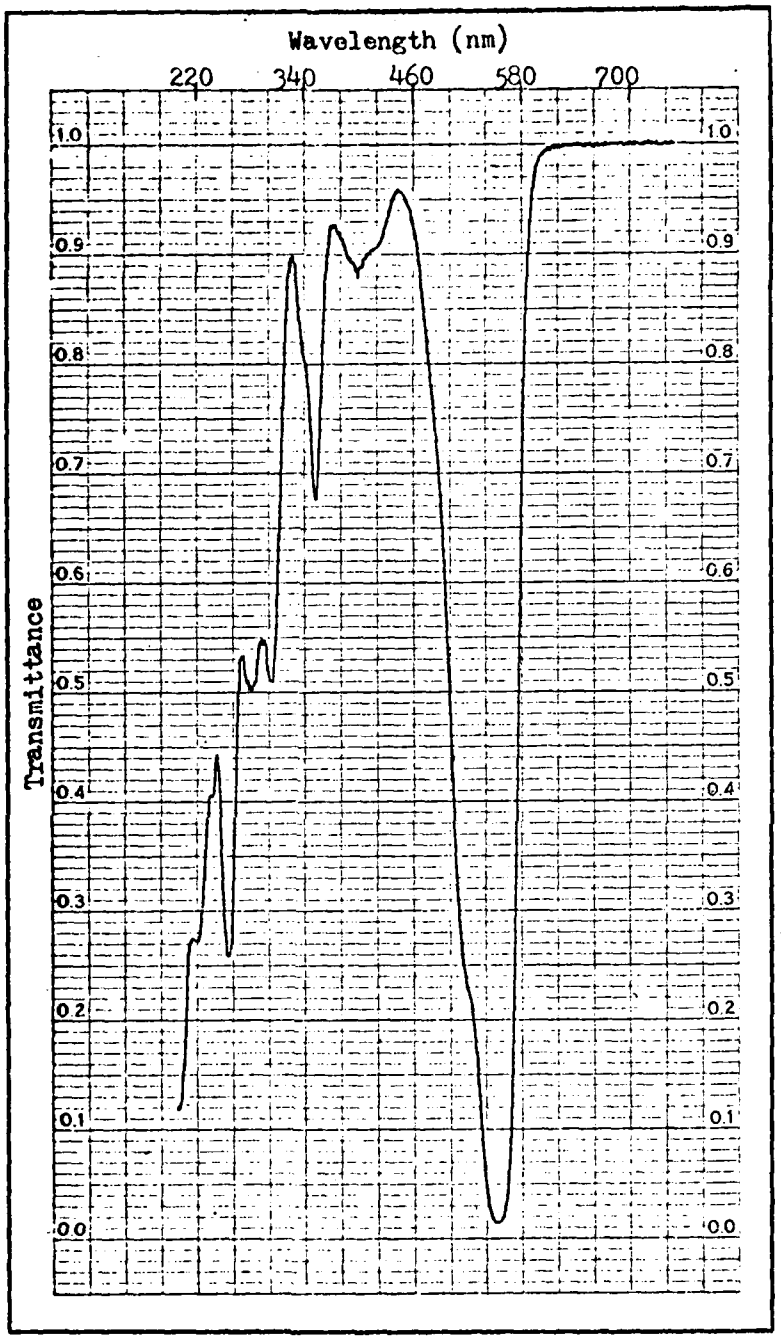

Fig. 8. UV-Visible Spectrum of Kiton Red S

the laser half-life was determined. The laser half-life is defined to be the number of shots required to reduce the beam energy to half of its initial value. Similarly, for the concentration versus shot number graphs, the concentration half-life is defined to be that number of shots at which the concentration of KRS is half of its initial value.

VI. Results and Discussion

Qualitative Results

Figures 9 and 10 show the UV spectra of ethanol and ethyl acetate.

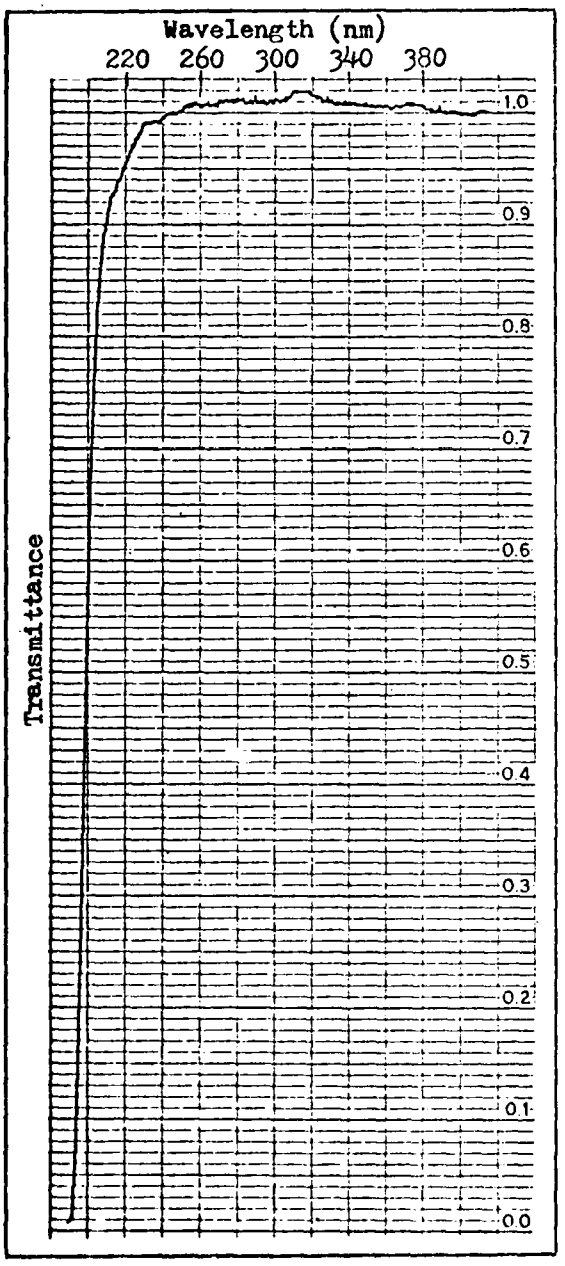

Fig. 9. UV Spectrum of Ethanol

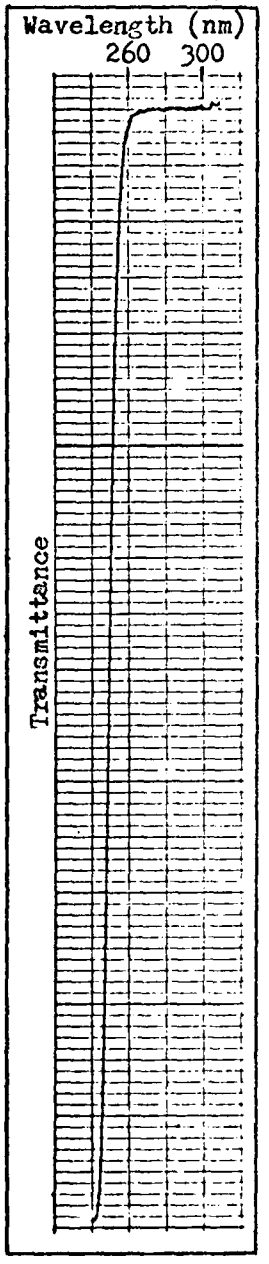

Fig. 10. UV Spectrum of Ethyl Acetate

These spectra indicate wavelength cutoffs of 192 nm and 244 nm for these two filter fluids, respectively. A UV spectrum of deionized water yields 100 percent transmittance down to 185 nm, the lower limit of the spectrophotometer. Thus, there is no wavelength cutoff for deionized water over the wavelength region of interest. A spectrum of the ethanol filter fluid after 5000 flashlamp pulses is pictured in Fig. 11. In comparing Figs. 9 and 11 it is clearly evident that the flashed ethanol begins to absorb UV radiation at higher wavelengths than the unflashed ethanol. This suggests a photolytic interaction of the flashlamp energy and the ethanol, in which products are produced which absorb energy between 200 nm and 300 nm.

In contrast with O'Brien's CW excitation results, none of the IR or UV-visible spectra of the degraded dye samples showed signs of functional group alteration over 5000 flashlamp pulses. No new peaks appeared and no existing peaks disappeared. Rather, those peaks with a KRS dependence decreased in size at the same relative rate, as the KRS concentration decreased. One possible exception can be seen in the UV spectrum of the dye sample withdrawn after 5000 shots of the first trial (Fig. 12). When compared with the undegraded-dye spectrum (Fig. 8), this figure shows the apparent loss of the peak at 280 nm. It may be, though, that the peak still exists but is masked by the shoulder at 270 nm.

In addition to the above results, a muddy orange color and a strong fruity smell were detected in the degraded samples of the first trial. The pleasant odor suggests the presence of a low molecular weight organic ester.

Quantitative Results

Figures 13 - 24 include plots of energy versus shot number and plots of IR-determined concentration versus shot number for all six photolysis

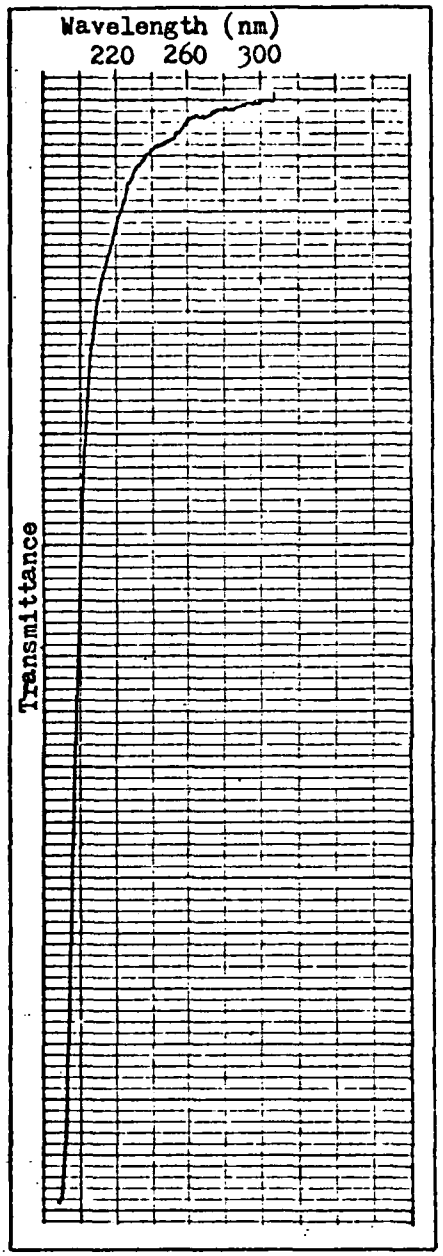

Fig. 11. UV Spectrum of Flashed Ethanol

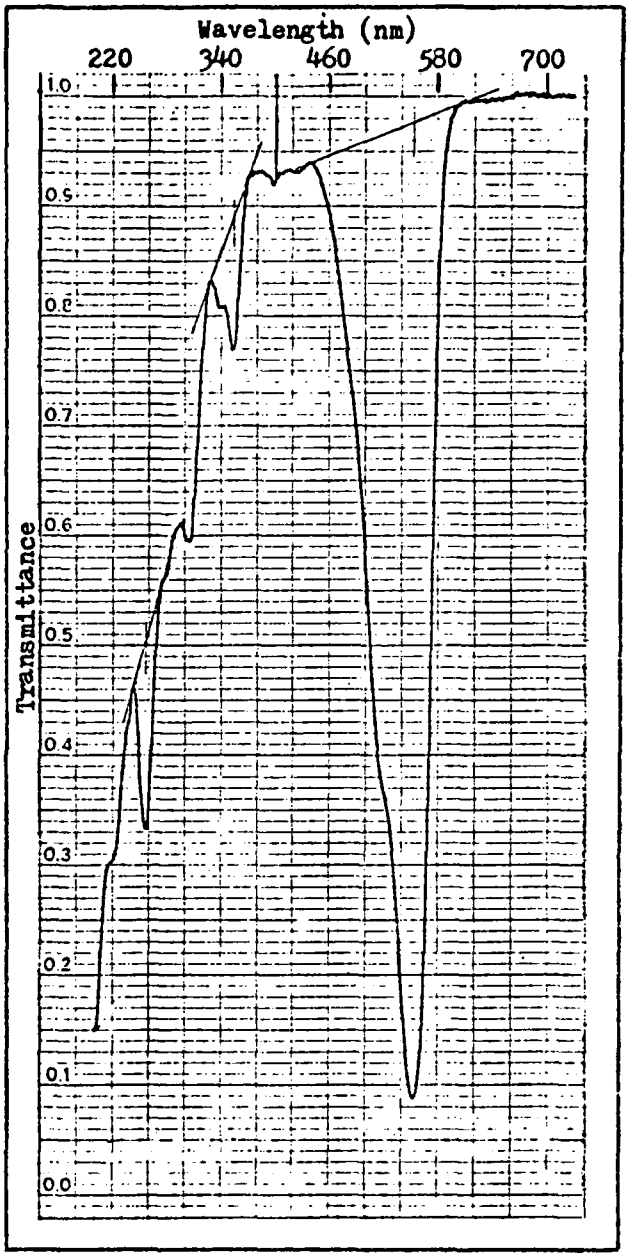

Fig. 12. UV Spectrum of Degraded Dye of Trial 1

trials. The data in tabular form is found in Appendix C. In Table II are found values for the initial beam energy, laser half-life, dye concentration half-life, and correlation coefficient for each trial.

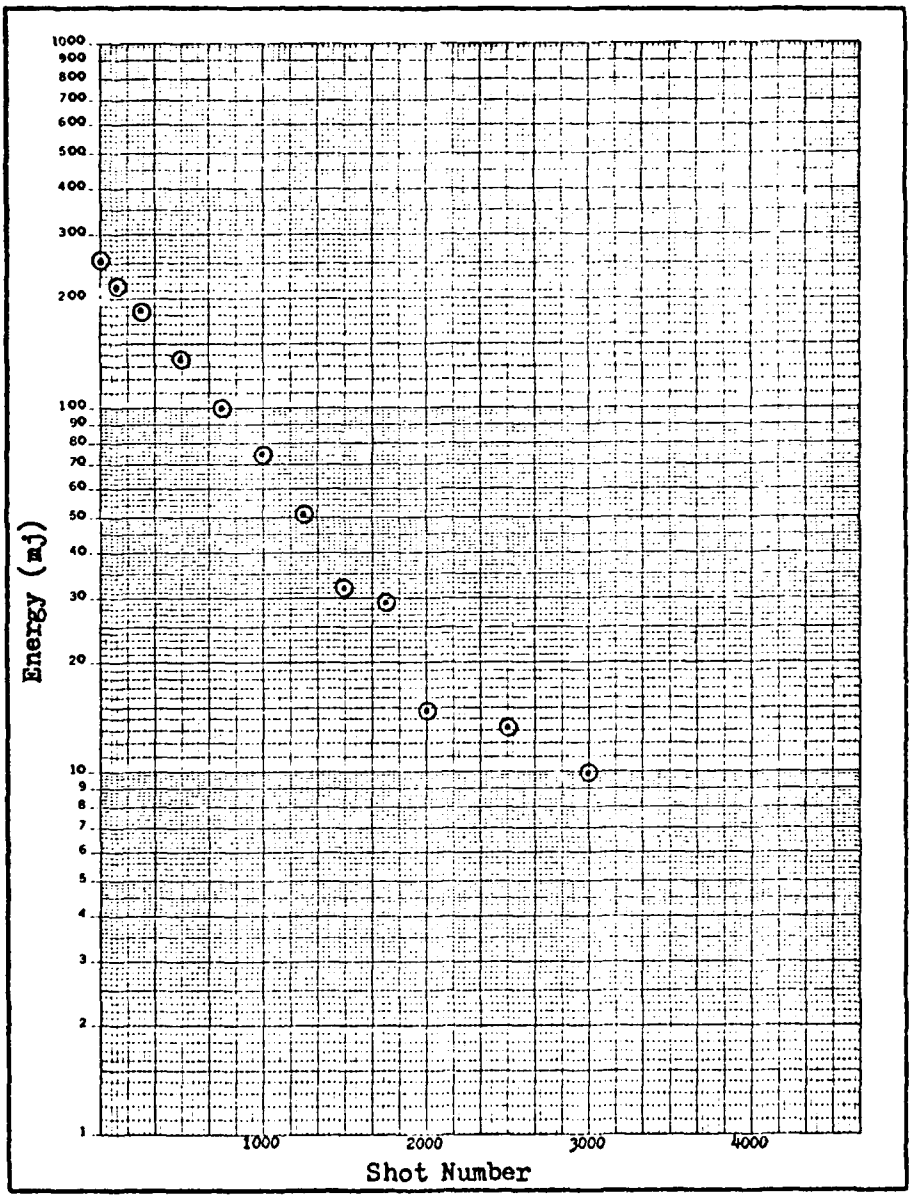

Fig. 13. Laser Energy Versus Shot Number for Trial 1

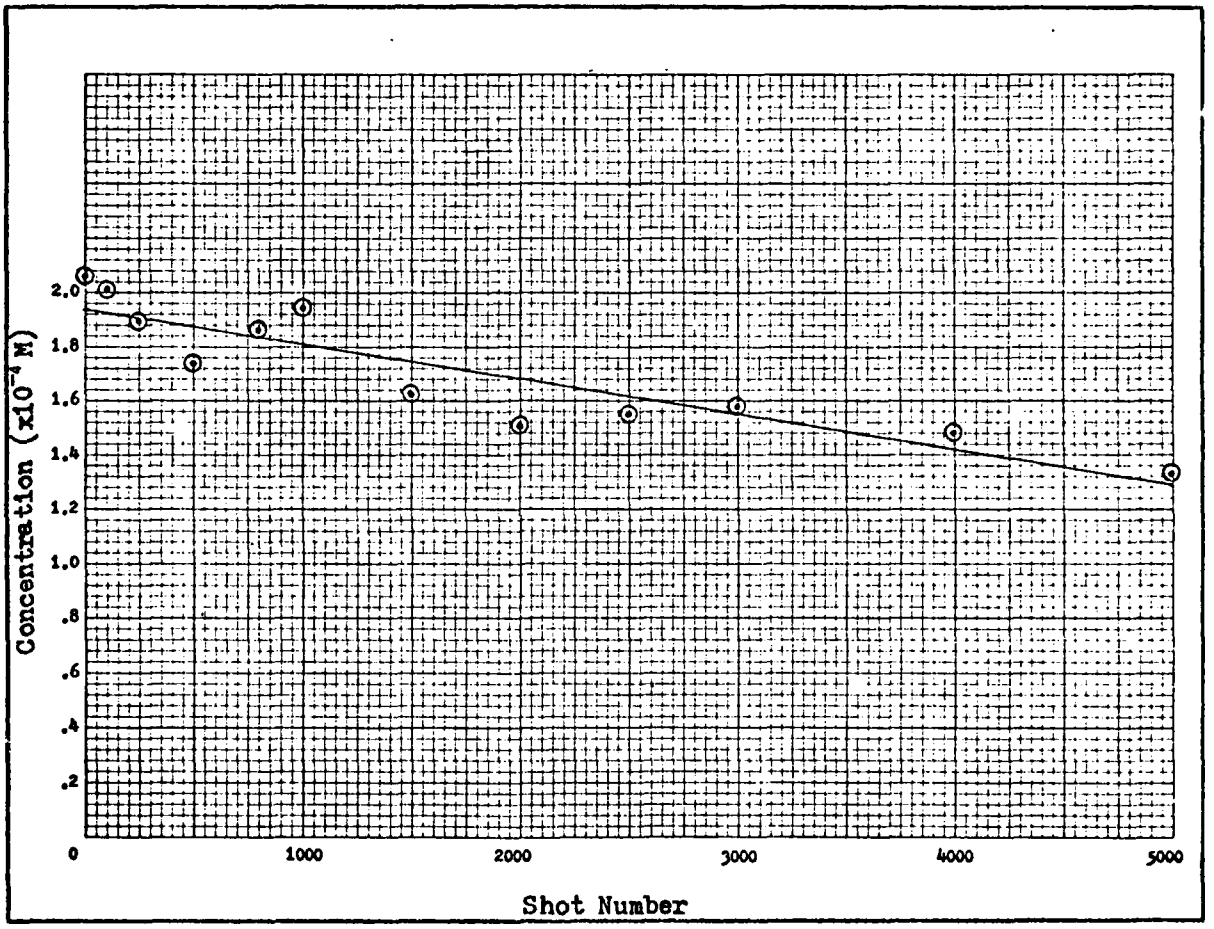

Fig. 14. Dye Concentration Versus Shot Number for Trial 1

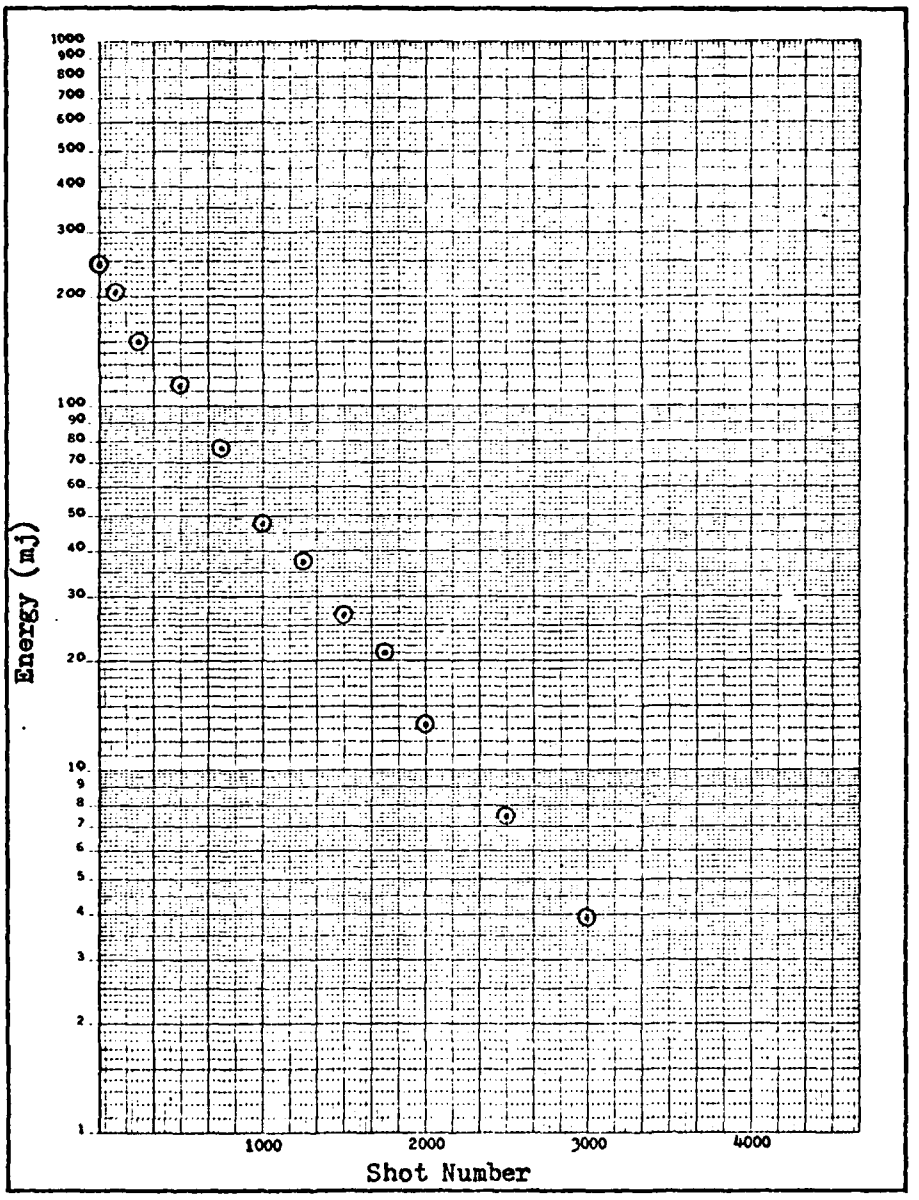

Fig. 15. Laser Energy Versus Shot Number for Trial 2

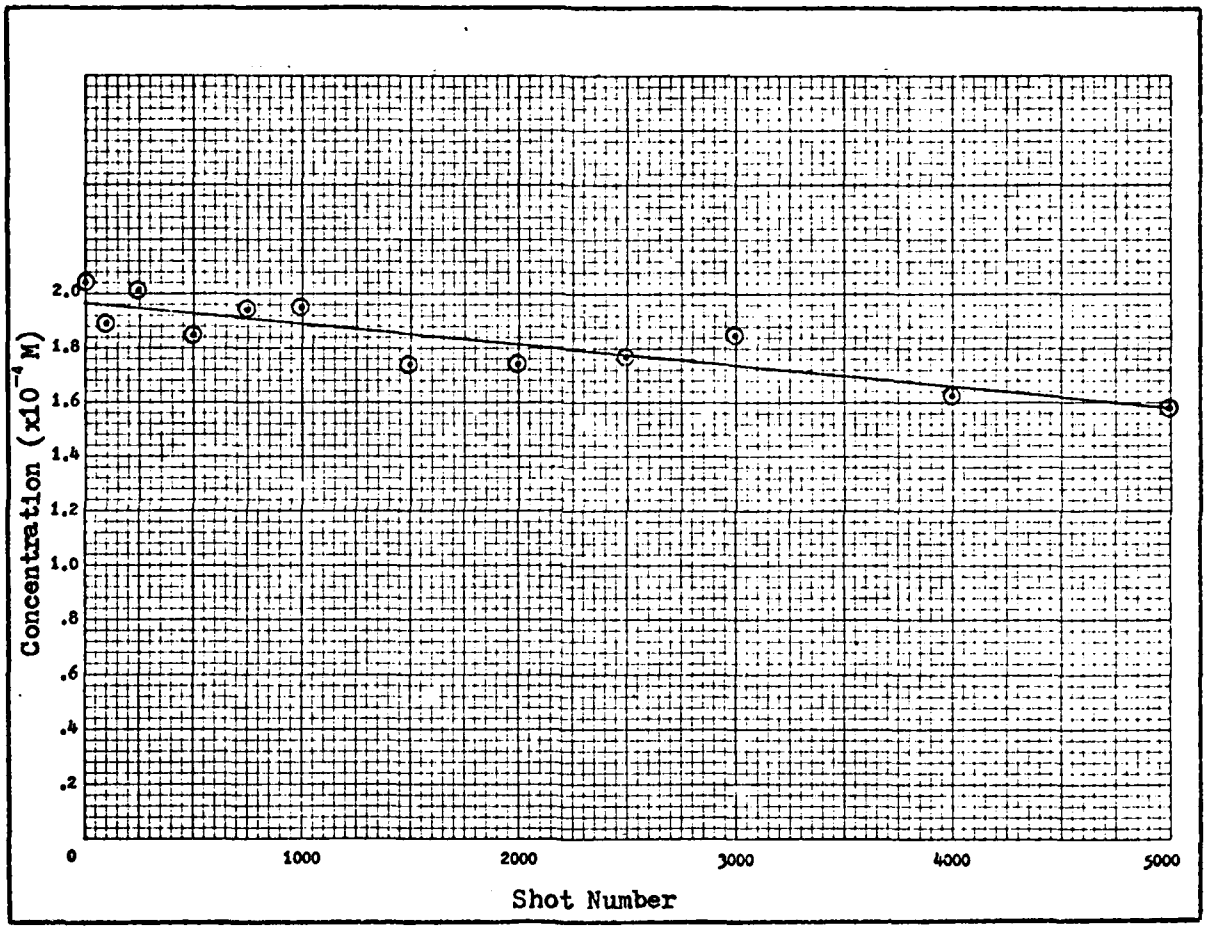

Fig. 16. Dye Concentration Versus Shot Number for Trial 2

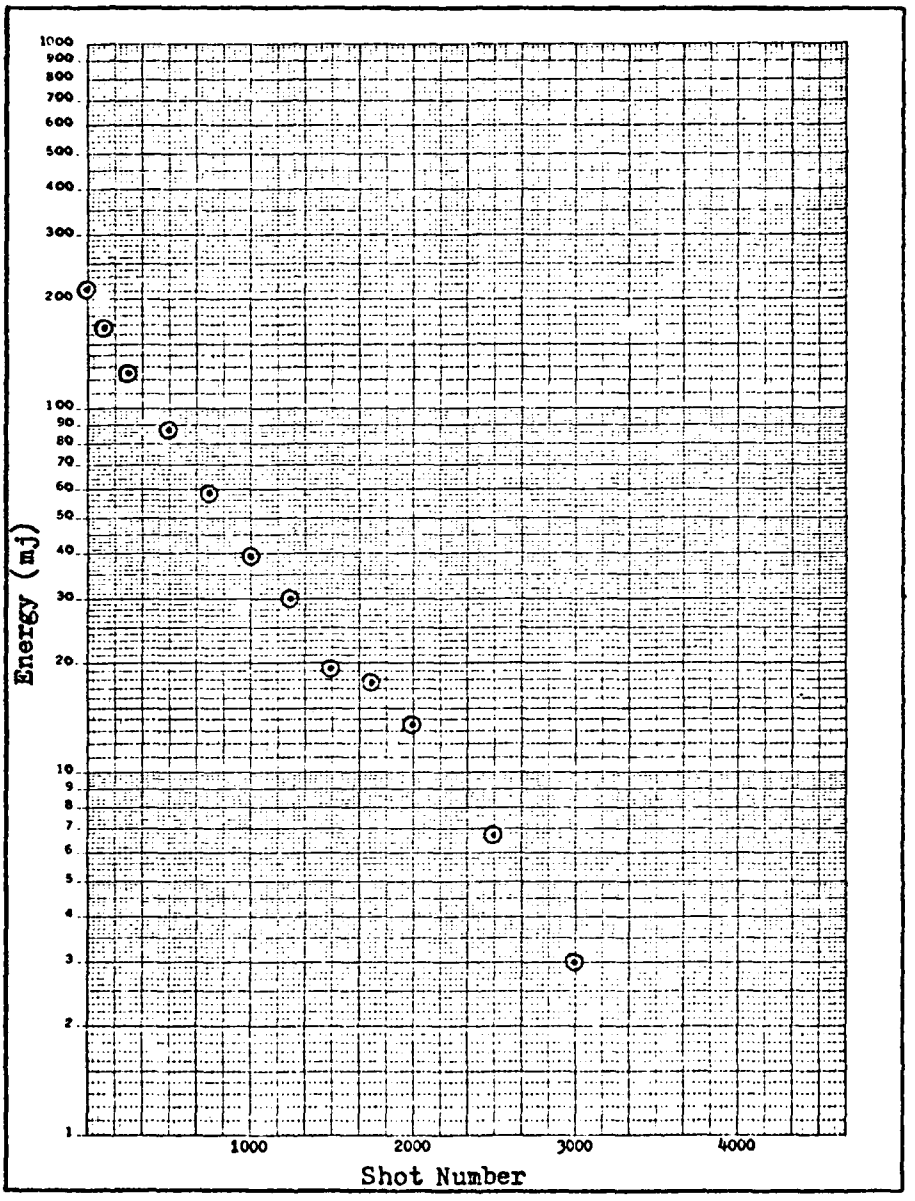

Fig. 17. Laser Energy Versus Shot Number for Trial 3

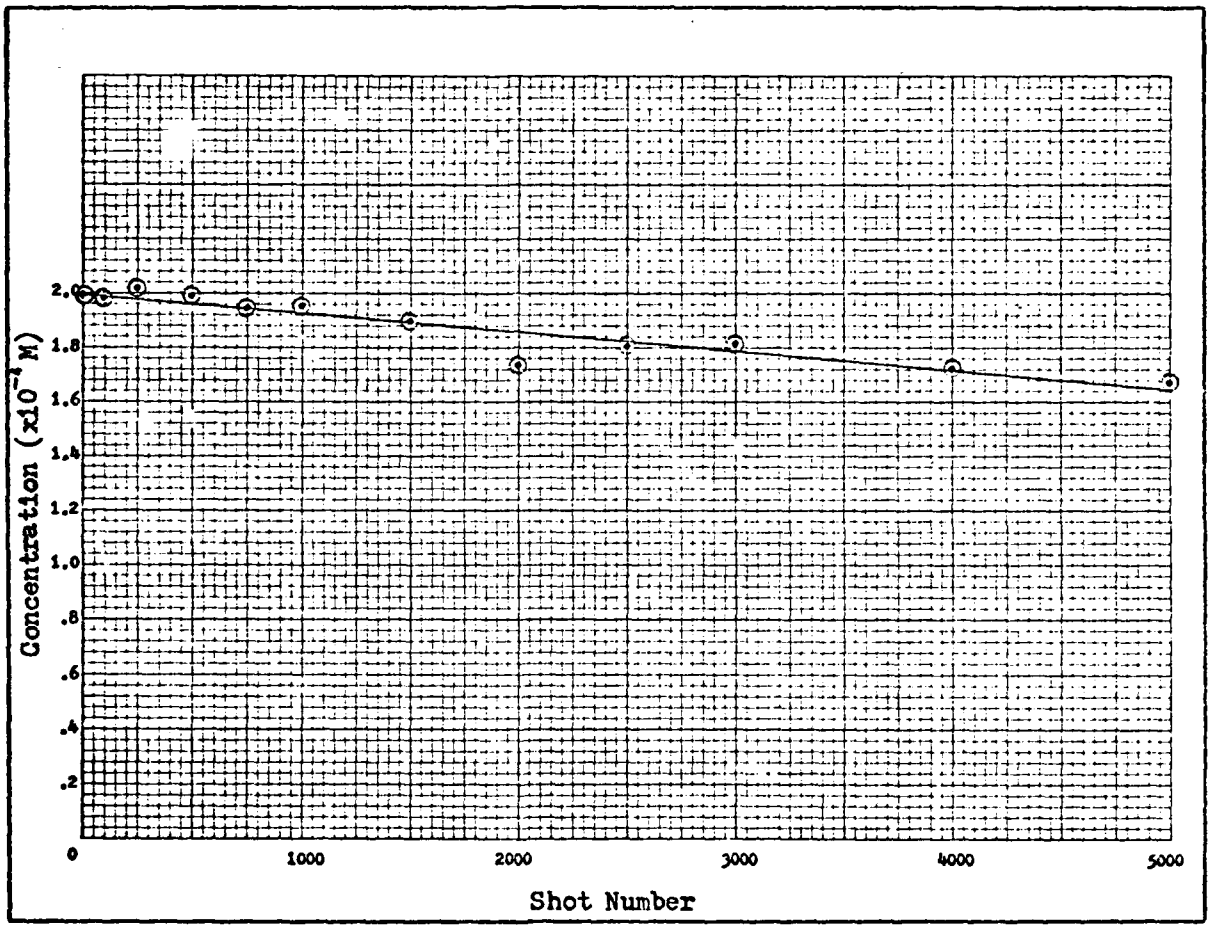

Fig. 18. Dye Concentration Versus Shot Number for Trial 3

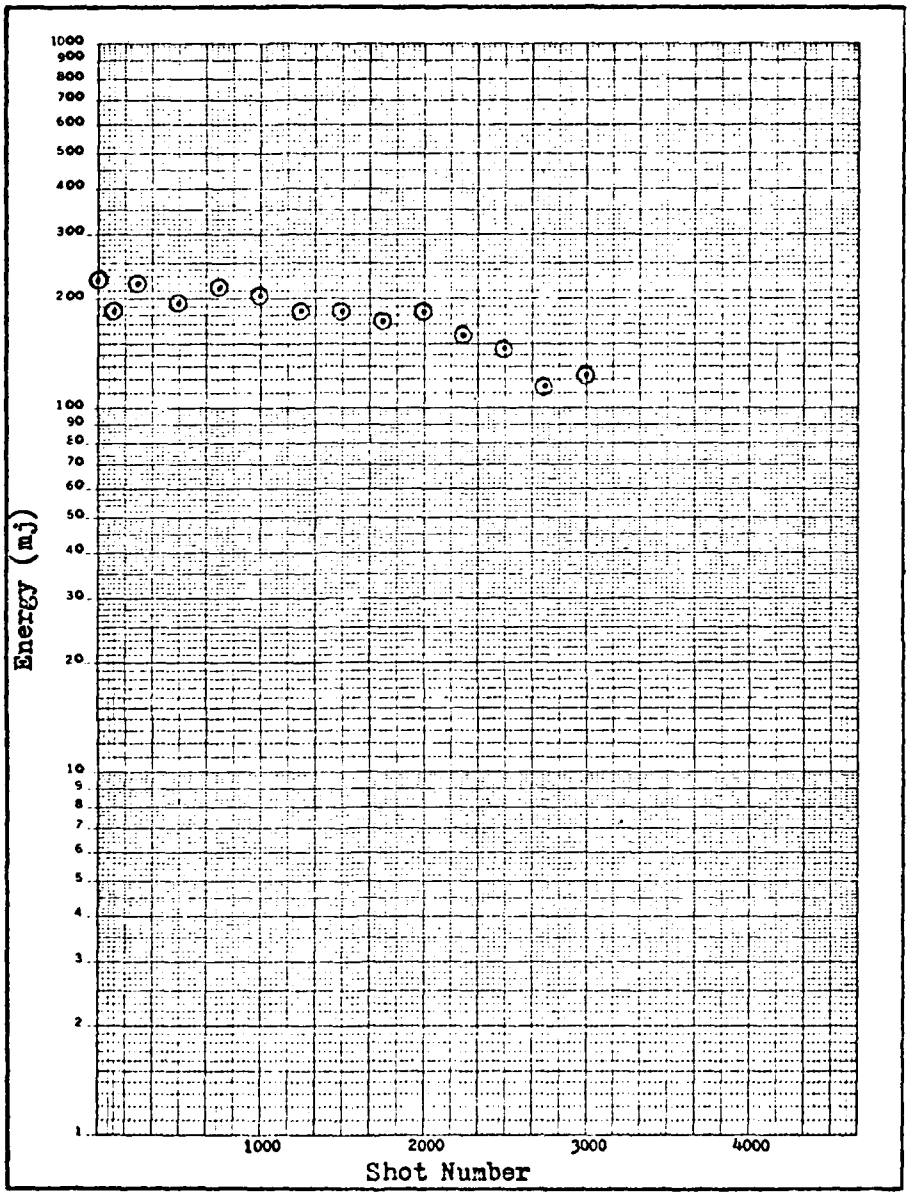

Fig. 19. Laser Energy Versus Shot Number for Trial 4

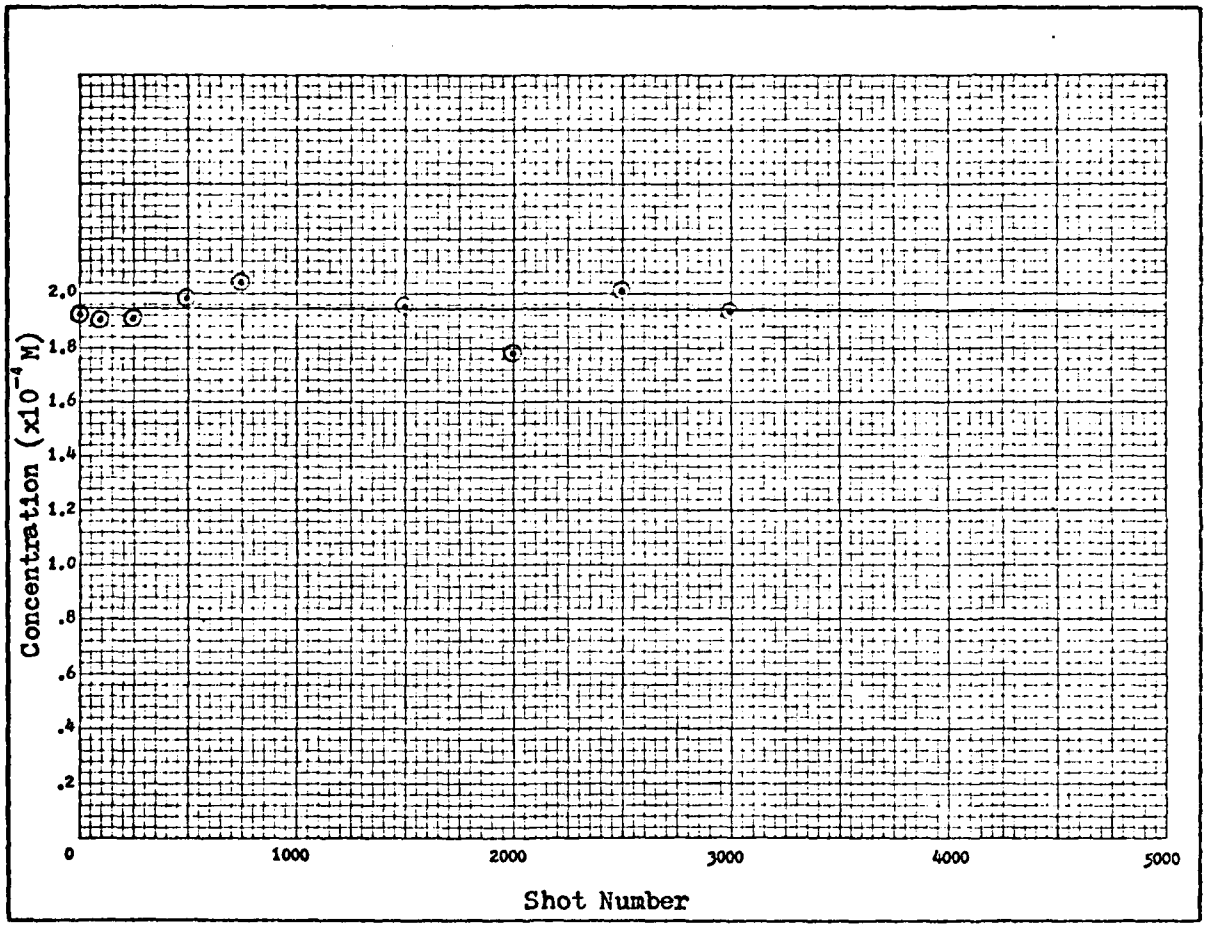

Fig. 20. Dye Concentration Versus Shot Number for Trial 4

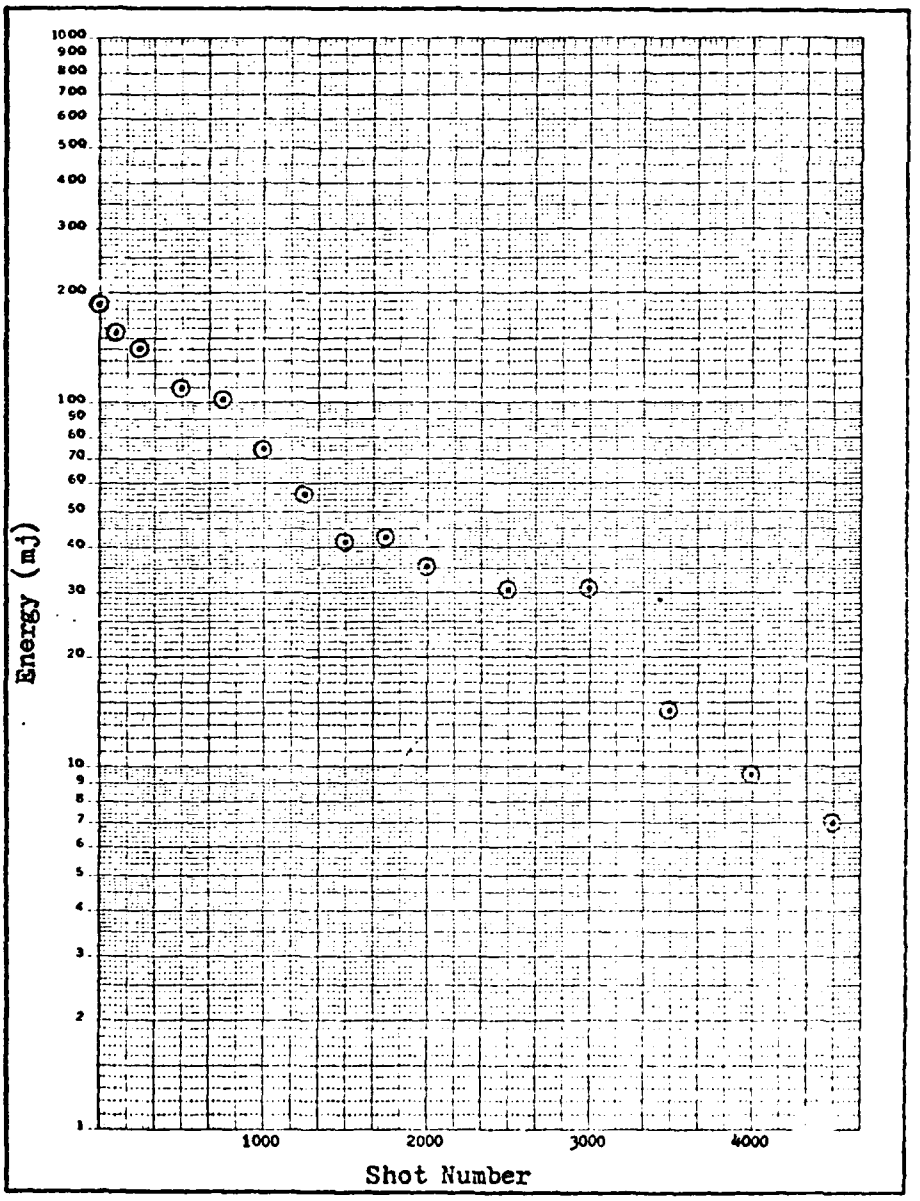

Fig. 21. Laser Energy Versus Shot Number for Trial 5

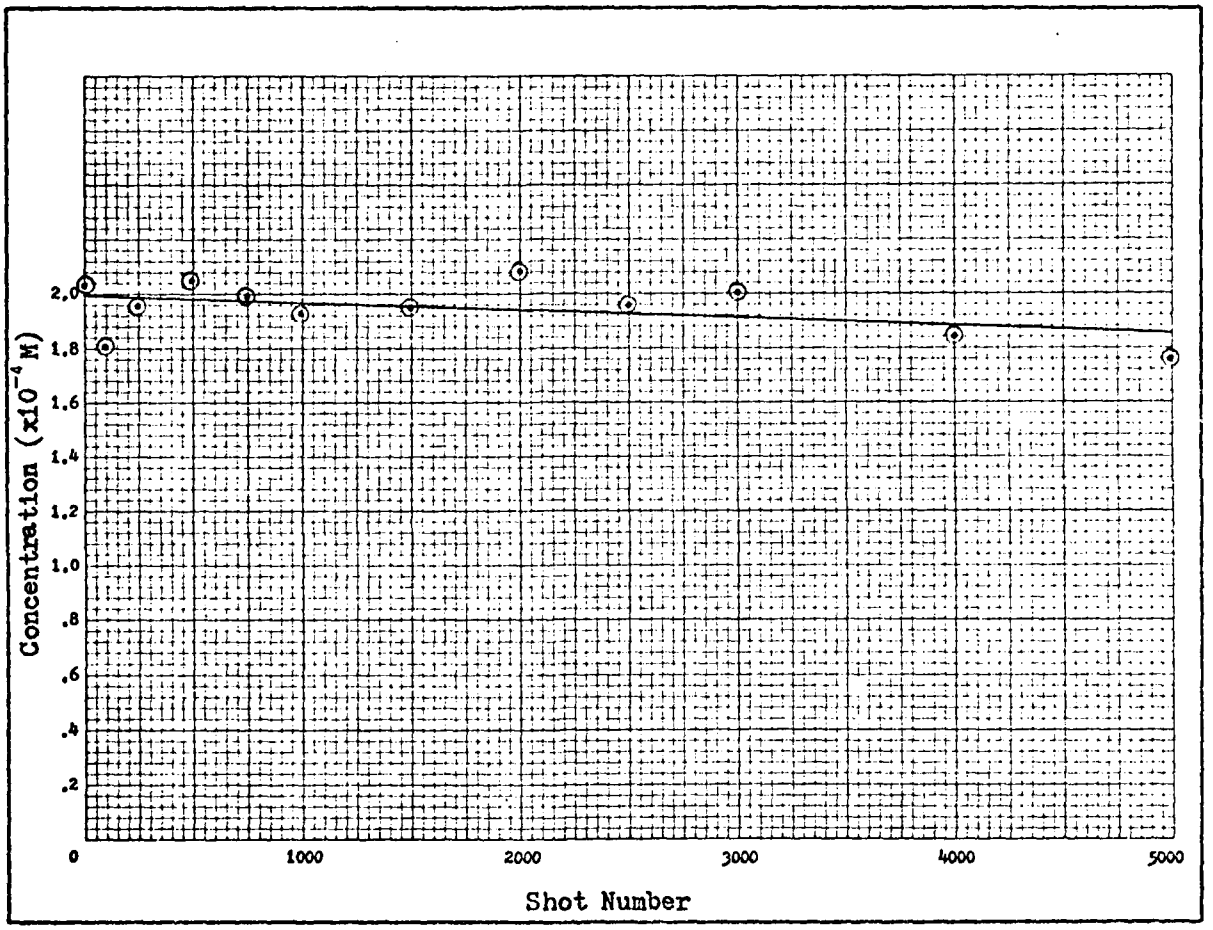

Fig. 22. Dye Concentration Versus Shot Number for Trial 5

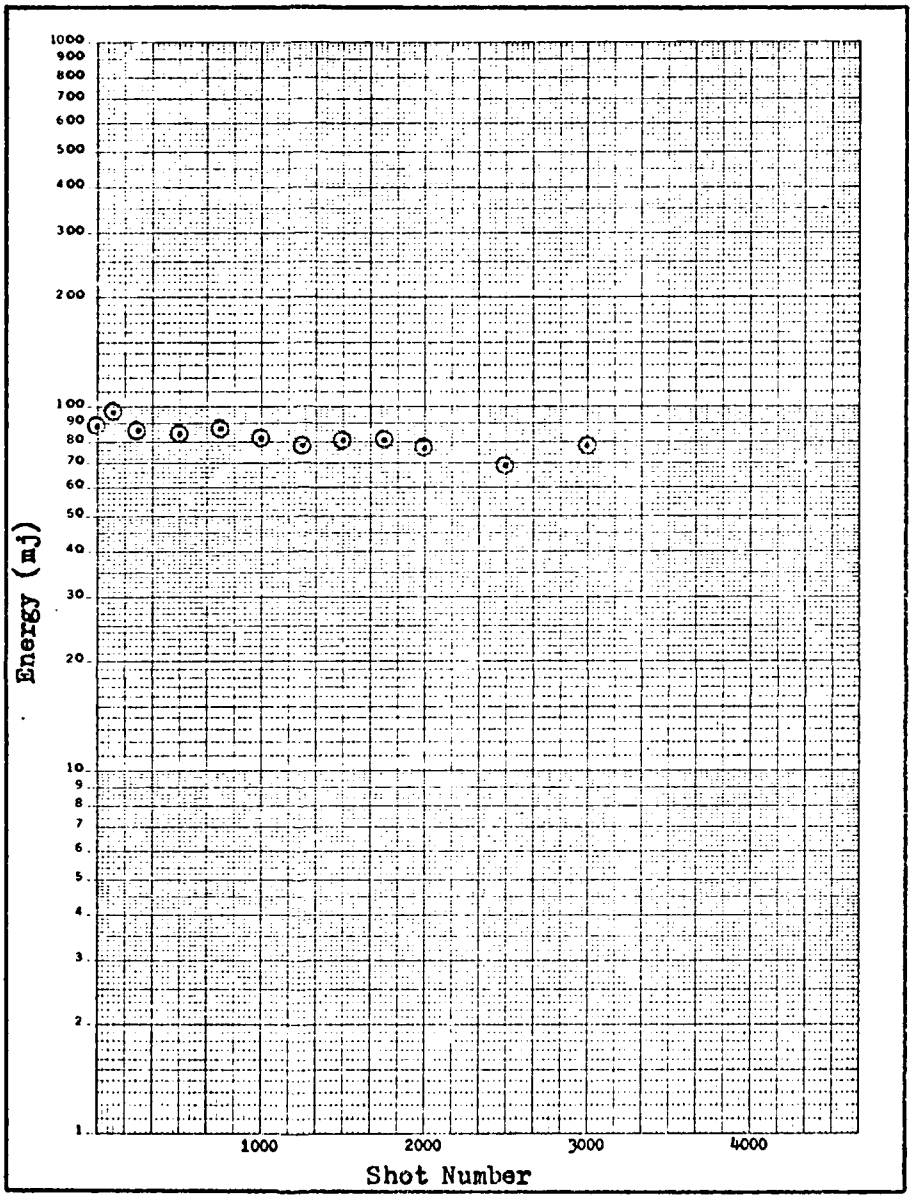

Fig. 23. Laser Energy Versus Shot Number for Trial 6

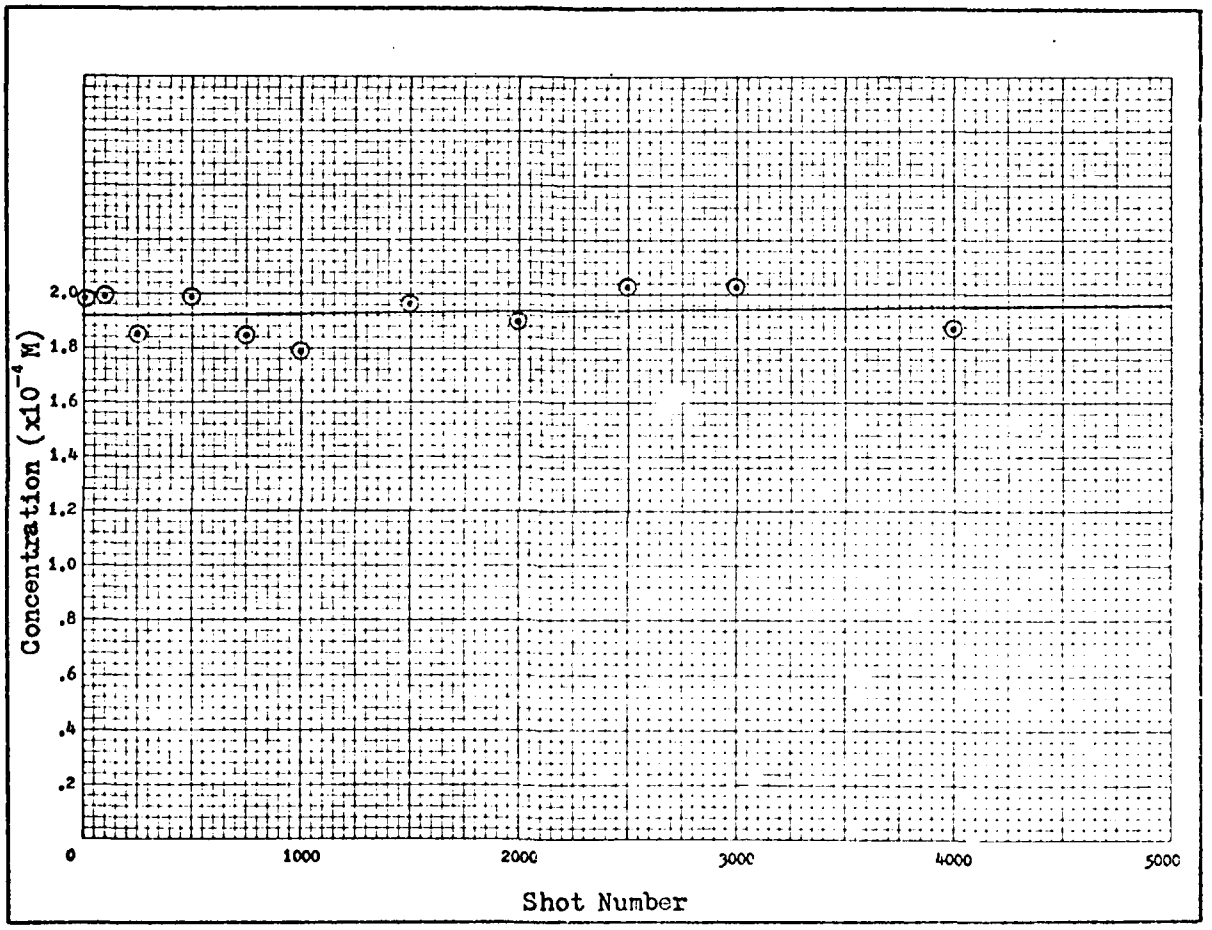

Fig. 24. Dye Concentration Versus Shot Number for Trial 6

Table II
Experimental Results

Trial	Filter Fluid	Cover Gas	Initial Beam Energy (mj)	Laser Half-life (# shots)	Concentration Half-life (# shots)	Correlation Coefficient
1	H_2O	Ar	250	550	7,400	0.90
2	H_2O	10.3% O_2	230	500	12,700	0.86
3	H_2O	21% O_2	200	450	14,300	0.93
4	EtOH	Ar	220	3,000	900,000	0.02
5	EtOH	21% O_2	180	750	35,200	0.46
6	EtAc	21% O_2	92	8,500	∞	0.12

In trials 1 through 3 the initial beam energy decreased only slightly (from 250 mj to 200 mj) as the oxygen concentration in solution was increased. Likewise, in trials 4 and 5 (where wavelengths less than 192 nm were obstructed from the dye) efficiency decreased 40 mj as the cover gas was changed from argon to air. In all five of these trials, the initial beam energies were quite acceptable. It is seen, however, that when wavelengths smaller than 244 nm were filtered from the dye (trial 6), the initial energy dropped by a factor of two. Obviously, those wavelengths between the cutoffs for ethanol and ethyl acetate are necessary for maximum efficiency.

Also apparent from Table II is the fact that in all six trials the dye concentration half-life was considerably greater than the laser half-life. In fact, for the first three trials lasing ceased between 3000 and 4000 shots, while the greatest dye-concentration loss (trial 1) was only 34 percent. This correspondence between a complete loss of laser energy and a comparatively small loss in dye concentration seems to indicate that energy output is not a function of dye concentration alone. This conclusion is supported by the fact that efficient lasing has been achieved with fresh dye solutions of concentration much less than that of the degraded samples (Ref 6:44-45). Apparently the photoreaction products are competing for the laser radiation or pump energy or both. It is not surprising that these photoproducts are not evident on the absorption spectra since it is likely that only small amounts are necessary to significantly affect the lasing characteristics.

The laser output energy decayed generally exponentially except for trial 1, where a break in the linearity occurred near shot 2000. Johnson reported a similar breakpoint in experiments with a coaxial laser and an argon cover gas. He postulated that there was an initial degradation due

to an impurity which was exhausted at the breakpoint, allowing for a slower degradation rate thereafter (Ref 17:20-22).

Oxygen played an important role in both beam energy degradation and dye degradation. It is clear from Table II that for either a water or an ethanol filter fluid, the presence of oxygen in solution acted to shorten the laser half-life. With an ethyl acetate filter fluid, whose cutoff is 244 nm, the laser energy degradation curve was virtually level. The effect of oxygen on the dye degradation rate was markedly dependent on the specific filter fluid used. When the full spectral range of the flashlamp was allowed to excite the dye solution (trials 1 - 3), the presence of oxygen in solution inhibited the rate of dye degradation. When wavelengths below 192 nm were eliminated from the dye cavity, though, the effect of oxygen was to accelerate the rate. And finally, when radiation below 244 nm was excluded, no decomposition occurred at all.

The degradation reaction under flashlamp conditions is zeroth order in KRS, as plots of KRS concentration versus shot number decrease linearly for all six trials. It can be concluded that KRS degradation is best modeled by Eq (11) in section II. The results for trials 1, 2, and 3 can be quantified by recalling that the rate expression

$$\frac{d\,[KRS]}{dS} = -\,K\,[KRS]^{o} \tag{16}$$

can be written as

$$\frac{d\,[KRS]}{dS} = -\,k\,[KRS]^{o}[O_2]^{a} \tag{17}$$

where k is the actual rate constant. K, the apparent rate constant, is simply the negative of the slope of the concentration versus shot

number curve for a particular trial. It includes an oxygen dependence term, as shown by the equation

$$K = k\,[O_2]^a \tag{18}$$

Knowing the slopes and oxygen concentrations for two different trials yields two simultaneous equations which can be solved to give values for the constants k and a. The concentration of dissolved oxygen is determined by using Henry's law, after Henry's law constant is calculated. These calculations are found in Appendix D. The numerical results for trials 2 and 3 are compiled in Table III. The rate expression for the

Table III
Numerical Results

Trial	Percent Oxygen in Cover Gas	Concentration of Dissolved Oxygen (mole/liter)	Apparent Rate Constant K (mole/liter-shot)
1	0	0	1.3×10^{-8}
2	10.3	1.0×10^{-3}	7.8×10^{-9}
3	21	2.1×10^{-3}	7.0×10^{-9}

Actual Rate Constant $k = 2.8 \times 10^{-9}$ mole/liter-shot

Exponent $a = -0.15$

case of a deionized water filter fluid can now be written

$$\frac{d\,[KRS]}{dS} = -2.8 \times 10^{-9}\,[KRS]^0\,[O_2]^{-0.15} \tag{19}$$

Only the IR-determined concentrations were used in constructing the concentration versus shot number plots, and in the kinetic analysis

above. There are two reasons for the decision to discount the reliability of the UV and visible data as accurate measures of KRS concentration. First, oftentimes the UV- and visible-determined concentrations differed markedly not only with one another, but with the IR-determined concentrations as well. Second, some of the data was ambiguous. To illustrate, Fig. 25 pictures the apparent-concentration versus shot number curve for

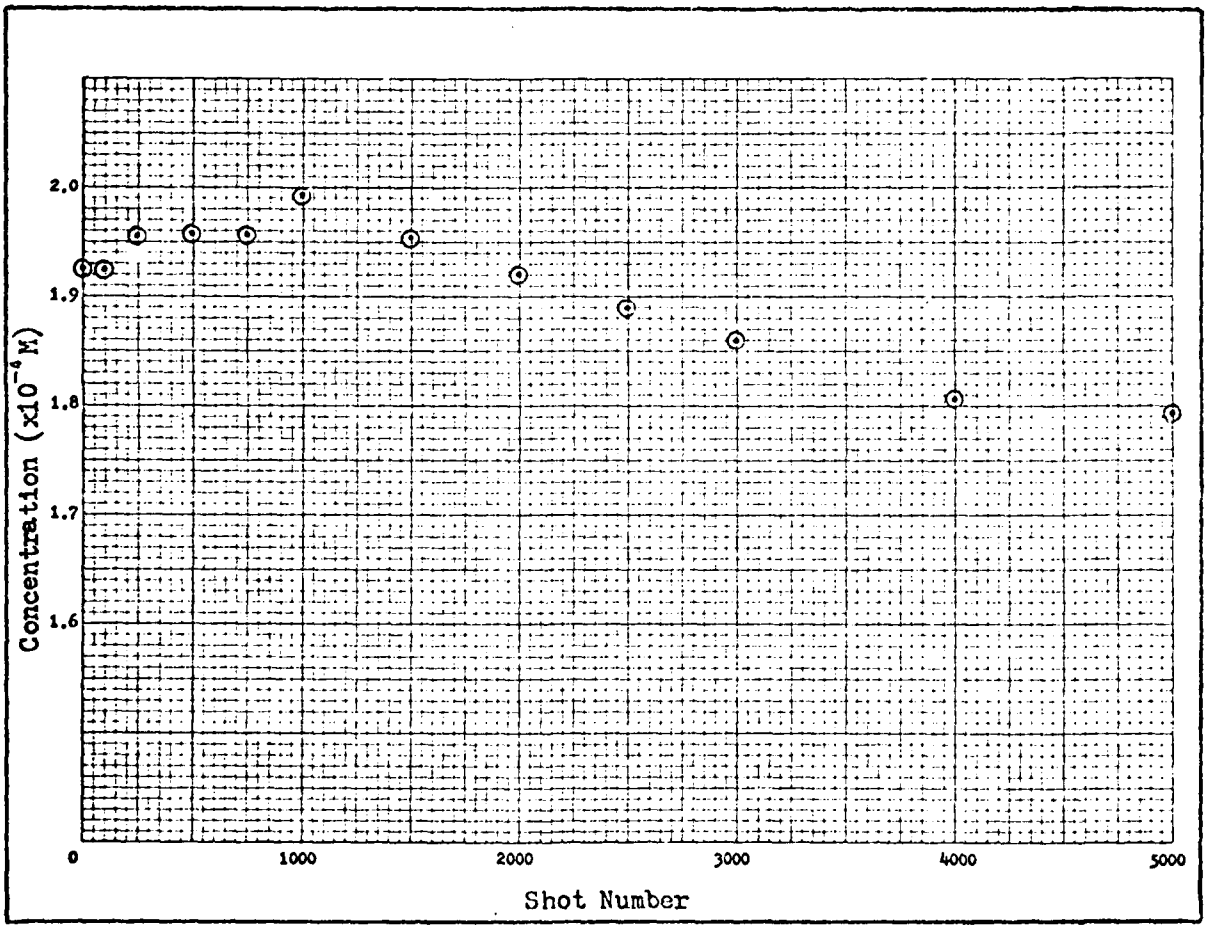

Fig. 25. UV-Determined Concentration Versus Shot Number for Trial 2

trial 2, which was obtained from measurements of the peak at 552 nm. A relative maximum is seen to appear in the curve. This would indicate a

rise in KRS concentration over the first 1000 shots if it were to be believed as an accurate measure. The inconsistent UV and visible results are possibly due to small amounts of impurities with large extinction coefficients and absorption characteristics similar to those of fresh dye solution. It is also possible that the reaction products absorb UV and visible radiation at the same wavelengths as the starting material does. Indeed, the initial rise in the spectrum shown in Fig. 25 points to the distinct possibility of intermediate formation.

General Discussion

From the results of this investigation it appears that there is a group of wavelengths less than 192 nm which, when allowed to excite the dye solution, causes oxygen to inhibit the dye degradation reaction (as shown in trials 1 - 3). When these wavelengths are excluded from the excitation process (as in trials 4 and 5) oxygen tends to increase the reaction rate.

Based upon the findings of this study, a reaction mechanism may now be proposed for the case of an ethanol solution of KRS under flashlamp excitation. Since the reaction is zeroth order in KRS, the dye concentration does not affect the reaction rate. When oxygen is present in solution and wavelengths less than 240 nm (the longest wavelength capable of oxygen dissociation) are allowed to excite the dye solution, molecular oxygen which is dissolved in solution is dissociated into atomic oxygen. This species then oxidizes the solvent to form free radicals which lead to products that absorb laser radiation or pump radiation. The rate of formation of these radicals, which are designated R_1, is dependent on the concentration of oxygen and on the excitation energy. By increasing either the amount of dissolved oxygen or the energy of excitation, the laser half-

life is shortened. This accounts for the exceptionally long half-life demonstrated in the sixth trial, where wavelengths smaller than 244 nm were obstructed. In this trial the oxygen in solution was unable to dissociate and act as an oxidant.

These R_1 radicals are similar to those found by Mostovnikov (Ref 23), who reported that illuminating the solvent alone (before mixing with the dye) had the same effect on efficiency as illuminating the dye and solvent together. The presence of these radicals is also arguable in light of Winters' conclusion that it is the presence of oxygen which leads to the production of the laser inhibiting substance (Ref 36:724).

The breakpoint in the energy versus shot number curve for trial 1, as well as the breakpoints discovered by Johnson (Ref 17:20-22), can be explained by the fact that argon does not displace all oxygen in solution. Therefore, R_1 radicals were formed until the point at which the oxygen in solution was scavenged, afterwhich the laser energy decreased at a sharply reduced rate. This also explains why no breakpoint was seen in the experiments where oxygen was bubbled into solution. As oxygen was never expended, the radicals continued to be formed.

There is a group of wavelengths less than 192 nm which induces free radical formation in the solvent. It is well known that at wavelengths between 180 nm and 190 nm, the $n \rightarrow \sigma^*$ transition occurs in alcohols (Ref 16:173). This transition may be the initial step in the pathway for radical formation. These radicals, designated R_2, are different than the R_1 radicals discussed above, in that they react with the triplet dye molecules to form fragments. However, they preferentially react with oxygen (over their rate of interaction with the dye) to create harmless intermediates not capable of reaction. Therefore, as the amount of oxy-

gen is increased, the degradation rate slows. In cases where oxygen is expended (as in trial 1), the rate accelerates as these R_2 radicals become available to react with the prevalent dye triplets. Two reports are consistent with this conclusion. Both Schwerzel (Ref 27) and Kato (Ref 18) found that for oxygen-saturated solutions, the degradation rate was rapidly accelerated after the oxygen in solution had been expended. In fact, Kato further observed that after the rate had accelerated, a fresh supply of oxygen acted to slow the rate once again.

If wavelengths less than 192 nm are not permitted to excite the dye solution, the R_2 radicals are not formed and oxygen alone influences the rate of degradation. The explanation is as follows. With light of sufficient energy to dissociate molecular oxygen, its role as oxidizer of the triplet dye molecules becomes more significant than its quenching role. Under these conditions, more oxygen in solution leads to accelerated dye degradation rates. When wavelengths less than 240 nm are excluded from the dye solution, however, molecular oxygen remains intact, and its triplet quenching role dominates. The dye then does not degrade, as evidenced by the sixth trial.

VII. Conclusion

For KRS in ethanol, the loss in laser beam energy is a function both of dye degradation and of the formation of two distinctly different radicals. One radical, R_1, leads to products which absorb laser energy, while the other, R_2, is reactive with the dye triplets.

To achieve maximum laser efficiency and minimum dye degradation, four conditions must be insured:

1. Wavelengths capable of forming the R_2 radicals must be excluded from the dye solution.

2. All wavelengths above those capable of forming the R_2 radicals must be included in the dye excitation process.

3. Dissolved oxygen must be replaced with a non-oxidizing triplet state quencher.

4. The photochemical products capable of absorbing laser radiation must be removed by appropriate filtration.

VIII. Recommendations

1. Those wavelengths capable of inducing the R_2 radical formation must be isolated.

2. Similar experiments should be performed with KBS in other solvents in order to confirm the proposed reaction mechanism. These should include solvents of similar polarity to ethanol but without the OH functional group, such as dimethylsulfoxide and dimethylformamide.

Bibliography

1. Adamson, Arthur W. A Textbook of Physical Chemistry. New York: Academic Press, 1973.

2. Allinger, Norman L. and Janet Allinger. Structures of Organic Molecules. New Jersey: Prentice-Hall, Inc., 1965.

3. Beer, D. and J. Weber. "Photobleaching of Organic Laser Dyes," Optics Communications, 5: 307-309 (July 1972).

4. Colthup, Norman B. et al. Introduction to Infrared and Raman Spectroscopy. New York: Academic Press, 1975.

5. Delahay, Paul. Instrumental Analysis. New York: The MacMillan Company, 1957.

6. Dorko, Ernest A. et al. Final Report, Degradation of KRS Under Flash and CW Irradiation. AFAL-TR-78-108. Wright-Patterson AFB, Ohio: Air Force Avionics Laboratory, 1978.

7. Drake, J. M. et al. "Kiton Red S and Rhodamine B. The Spectroscopy and Laser Performance of Red Laser Dyes," Chemical Physics Letters, 35: 181-188 (September 1975).

8. Drexhage, K. H. "Structure and Properties of Laser Dyes," Topics in Applied Physics, Dye Lasers, edited by F. P. Schafer. New York: Springer Verlag, 1973.

9. Eshbach, Ovid W. Handbook of Engineering Fundamentals (Second edition). New York: John Wiley & Sons, Inc., 1966.

10. Fletcher, Aaron N. Near-Ultraviolet Lasing Dyes. Part 2. Effects of Coaxial Flashlamp Excitation. NWC TP 5768, Part 2. China Lake, California: Naval Weapons Center, 1975.

11. Fritz, J. S. and G. S. Hammond. Quantitative Organic Analysis. New York: John Wiley & Sons, Inc., 1957.

12. Frost, Arthur A. and Ralph G. Pearson. Kinetics and Mechanism. New York: John Wiley & Sons, Inc., 1961.

13. Herzberg, Gerhard. Molecular Spectra and Molecular Structure: Spectra of Diatomic Molecules (Second edition). New York: Van Nostrand Reinhold Company, 1950.

14. Hewlett-Packard HP-25 Applications Programs. Cupertino, California: Hewlett-Packard Company, 1975.

15. Ippen, E. P. et al. "Rapid Photobleaching of Organic Laser Dyes in Continuously Operated Devices," IEEE Journal of Quantum Electronics, 7: 178-179 (April 1971).

16. Jaffe', H. H. and Milton Orchin. Theory and Applications of Ultraviolet Spectroscopy. New York: John Wiley & Sons, Inc., 1962.

17. Johnson, Sidney L., Jr. Kiton Red S Lifetime Studies. AFAL-TR-77-209. Wright Patterson AFB, Ohio: Air Force Avionics Laboratory, 1977.

18. Kato, Daisuke and Akira Sugimura. "Deterioration of Rhodamine 6G Dye Solution in Methanol," Optics Communications, 10: 327-330 (April 1974).

19. Keller, Richard A. "Effect of Quenching of Molecular Triplet States in Organic Dye Lasers," IEEE Journal of Quantum Electronics, 6: 411-416 (July 1970).

20. Korobov, V. E. et al. "Effect of Spectral Composition of Pumping on Mechanism of Rhodamine 6G Photoreactions," translated from Zhurnal Prikladnoi Spektroskopii, 26: 841-843 (May 1977).

21. Levin, M. B. and M. I. Snegov. "Effect of Photoreaction Products on Spontaneous and Stimulated Emission of Alcoholic Solutions of Rhodamine 6G," Optics and Spectroscopy, 38: 532-533 (May 1975).

22. Marling, J. B. et al. "Chemical Quenching of the Triplet State in Flashlamp-Excited Liquid Organic Lasers," Applied Physics Letters, 17: 527-530 (December 1970).

23. Mostovnikov, V. A. et al. "Recovery of Lasing Properties of Dye Solutions After Their Photolysis," Soviet Journal of Quantum Electronics, 6: 1126-1128 (September 1976).

24. Neister, S. Edward. "The Dye Laser Dye Update," Optical Spectra: 34-36 (February 1977).

25. O'Brien, Kevin. Kinetics and Wave Length Dependence of the Photolytic Degradation of Kiton Red-S Laser Dye. AFIT Thesis, AFIT/GEP/AA/77D-2. Wright-Patterson AFB, Ohio: Air Force Institute of Technology, 1977.

26. Schafer, F. P. "Principles of Dye Laser Operation," Topics in Applied Physics, Dye Lasers, edited by F. P. Schafer. New York: Springer Verlag, 1973.

27. Schwerzel, Robert E., research scientist for Battelle Laboratories, Columbus, Ohio. Oral presentation given at the Air Force Avionics Laboratory, September 7, 1978.

28. Shank, C. V. "Physics of Dye Lasers," Reviews of Modern Physics, 47: 649-657 (July 1975).

29. Skinner, Gordon B. Introduction to Chemical Kinetics. New York: Academic Press, 1974.

30. Teschke, O. et al. "Theory and Operation of High-Power CW and Long-Pulse Dye Lasers," IEEE Journal of Quantum Electronics, 12: 383-395 (July 1976).

31. Wang, Harry H. L. and Christopher H. Taji. "The Negative Effect of Cyclooctatetraene on Small Coaxial Flashlamp-Pumped Dye Lasers," IEEE Journal of Quantum Electronics, 13: 85-86 (March 1977).

32. Warden, J. T. and Lucille Gough. "Flashlamp-Pumped Laser Dyes: A Literature Survey," Applied Physics Letters, 19: 345-348 (November 1971).

33. Washburn, Edward W., ed. International Critical Tables of Numerical Data, Physics, Chemistry, and Technology, III. New York: McGraw-Hill Book Company, 1928.

34. Weast, Robert C., ed. Handbook of Chemistry and Physics (53rd edition). Cleveland, Ohio: The Chemical Rubber Publishing Company, 1972.

35. Weber, J. "Continuously UV-Bleaching of Organic Laser Dyes," Physics Letters, 45A: 35-36 (August 1973).

36. Winters, B. H. et al. "Photochemical Products in Coumarin Laser Dyes," Applied Physics Letters, 25: 723-724 (December 1974).

37. Yamashita, Mikio and Hiroshi Kashiwagi. "Photodegradation Mechanisms in Laser Dyes: A Laser Irradiated ESR Study," IEEE Journal of Quantum Electronics, 12: 90-95 (February 1976).

Additional References

1. Allinger, Norman L. et al. Organic Chemistry. New York: Worth Publishers, Inc., 1971.

2. Herz, Werner. The Shape of Carbon Compounds. New York: W. A. Benjamin, Inc., 1964.

3. McCullough, Andrew W. Dye Laser Beam Quality Improvement. AFAL-TR-77-140. Wright-Patterson AFB, Ohio: Air Force Avionics Laboratory, 1977.

4. Sax, N. Irving. Dangerous Properties of Industrial Materials. New York: Van Nostrand Reinhold Company, 1975.

5. Walling, Cheves. Free Radicals in Solution. New York: John Wiley & Sons, Inc., 1957.

Appendix A

Calibration Curves

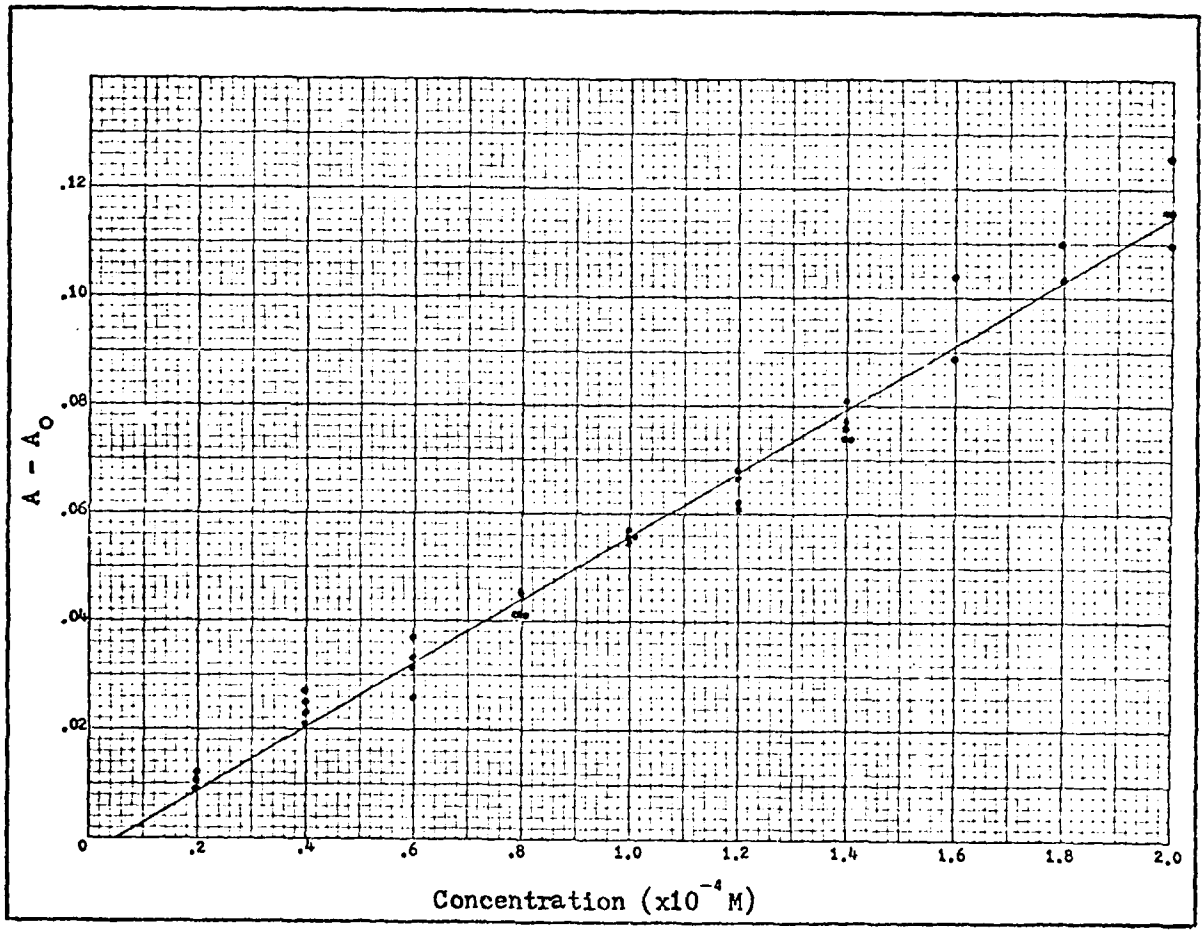

Fig. 26. IR Calibration Curve

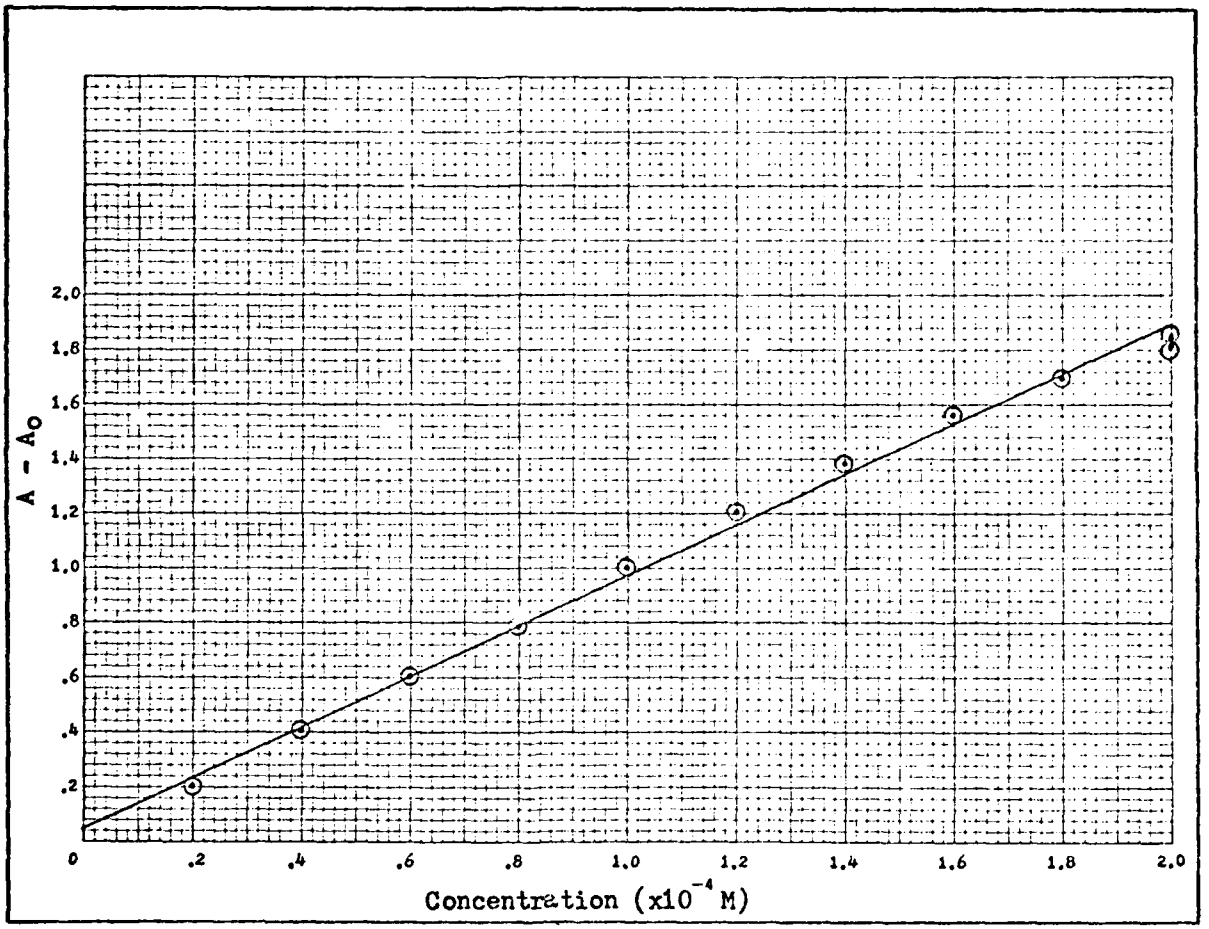

Fig. 27. Visible Calibration Curve

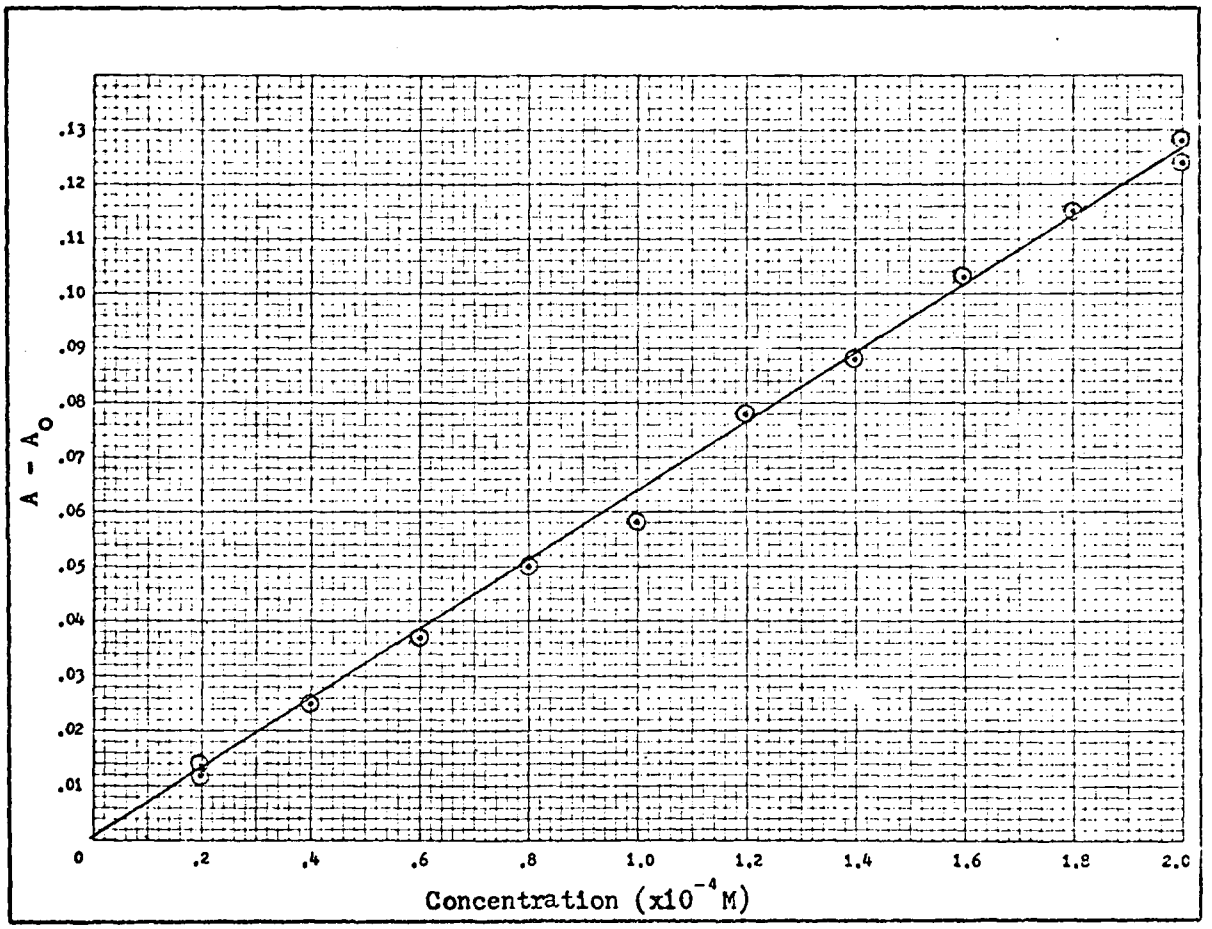

Fig. 28. UV Calibration Curve

Appendix B

Conversion of Peak Size to Concentration

Sample Calculation

Conversion of Peak Size to Concentration

Sample Calculation

As shown in Fig. 29, a tie-line is drawn across the shoulders of the peak at 7.5μ. The absorbance at the tie-line (at the peak wavelength) is designated A_o, and is seen to equal 0.051. The absorbance at the bottom of the peak, A, is 0.160. The difference $A - A_o$ is 0.109, which, from the calibration curve (Fig. 26), corresponds to a KRS concentration of 1.896×10^{-4} M.

This procedure was accomplished for all IR spectra in a trial, and the concentration of KRS was plotted against shot number. A linear regression was performed by the method of least squares, yielding the y-intercept, the slope, and the coefficient of determination r^2 (Ref 14: 87-91). The correlation coefficient r was then determined (Ref 9:2.30-2.31).

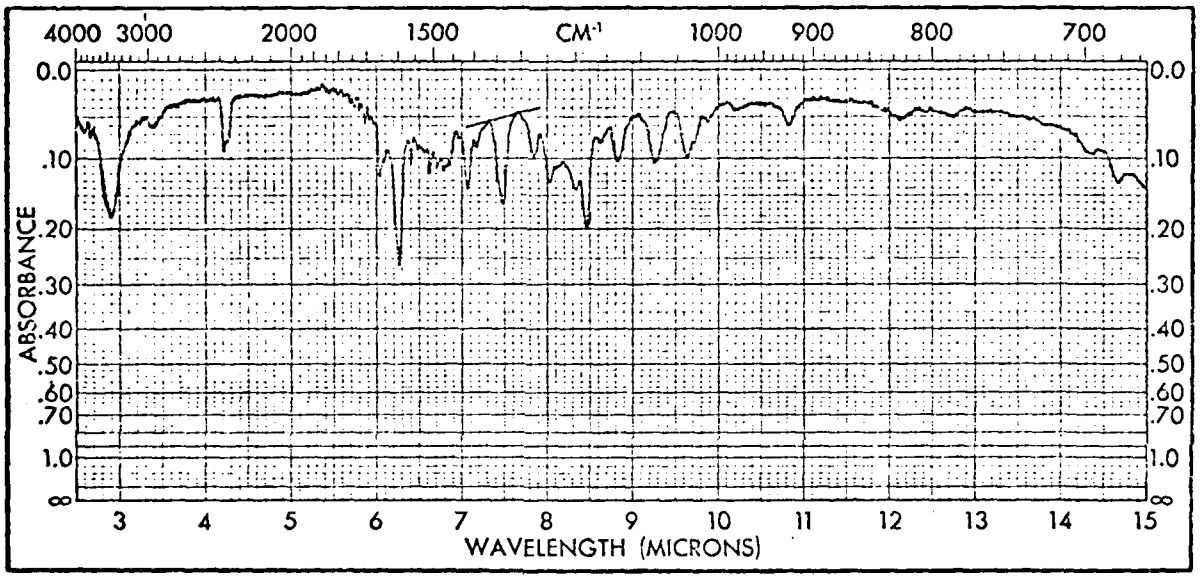

Fig. 29. IR Spectrum of Partially Degraded Kiton Red S

Appendix C

Tabular Data

Table IV
Data from IR Calibration Curve

Concentration ($x10^{-4}$ M)	A_o	A	$A - A_o$
2.0	0.036	0.152	0.116
2.0	0.046	0.156	0.110
2.0	0.047	0.163	0.116
2.0	0.050	0.176	0.126
1.8	0.050	0.160	0.110
1.8	0.050	0.153	0.103
1.6	0.041	0.130	0.089
1.6	0.038	0.142	0.104
1.4	0.039	0.120	0.081
1.4	0.037	0.113	0.076
1.4	0.048	0.125	0.077
1.4	0.044	0.118	0.074
1.4	0.044	0.118	0.074
1.2	0.031	0.092	0.061
1.2	0.028	0.090	0.062
1.2	0.037	0.105	0.068
1.2	0.031	0.098	0.067
1.0	0.033	0.089	0.056
1.0	0.038	0.093	0.055
1.0	0.037	0.094	0.057
1.0	0.036	0.092	0.056
0.8	0.029	0.070	0.041

Table IV (Continued)

Concentration ($x10^{-4}$ M)	A_o	A	$A - A_o$
0.8	0.027	0.068	0.041
0.8	0.034	0.079	0.045
0.8	0.026	0.067	0.041
0.6	0.040	0.073	0.033
0.6	0.040	0.066	0.026
0.6	0.035	0.072	0.037
0.6	0.027	0.059	0.032
0.4	0.027	0.050	0.023
0.4	0.031	0.058	0.027
0.4	0.044	0.069	0.025
0.4	0.027	0.048	0.021
0.2	0.025	0.036	0.011
0.2	0.012	0.024	0.012
0.2	0.019	0.028	0.009

y-intercept = -0.003

slope = 590

r^2 = 0.98

Table V
Data from Visible Calibration Curve

Concentration ($x10^{-4}$ M)	T_o	A_o	T	A	$A - A_o$
2.0	0.982	0.008	0.014	1.854	1.846
2.0	0.981	0.008	0.015	1.824	1.816
1.8	0.984	0.007	0.020	1.699	1.692
1.6	0.985	0.007	0.027	1.569	1.562
1.4	0.987	0.006	0.041	1.387	1.382
1.2	0.990	0.004	0.062	1.208	1.203
1.0	0.990	0.004	0.097	1.013	1.009
0.8	0.992	0.003	0.163	0.788	0.784
0.6	0.993	0.003	0.248	0.606	0.602
0.4	0.996	0.002	0.392	0.407	0.405
0.2	0.997	0.001	0.622	0.206	0.205
0.2	0.994	0.003	0.623	0.206	0.203

y-intercept = 0.051

slope = 9160

$r^2 = 1.00$

Table VI
Data from UV Calibration Curve

Concentration ($x10^{-4}$ M)	T_o	A_o	T	A	$A - A_o$
2.0	0.917	0.038	0.689	0.162	0.124
2.0	0.915	0.039	0.681	0.167	0.128
1.8	0.928	0.032	0.712	0.148	0.115
1.6	0.931	0.031	0.735	0.134	0.103
1.4	0.948	0.023	0.774	0.111	0.088
1.2	0.954	0.020	0.798	0.098	0.078
1.0	0.961	0.017	0.840	0.076	0.058
0.8	0.967	0.015	0.862	0.064	0.050
0.6	0.980	0.009	0.901	0.045	0.037
0.4	0.987	0.006	0.932	0.031	0.025
0.2	0.980	0.009	0.952	0.021	0.013
0.2	0.979	0.009	0.953	0.021	0.012

y-intercept = 0.001

slope = 638

$r^2 = 1.00$

Table VII
Data from Trial 1

# Shots	Laser Beam Energy (mj)	$A - A_o$	Concentration ($x10^{-4}$ M)
0	251	0.119	2.07
100	215	0.116	2.01
250	186	0.109	1.90
500	136	0.100	1.74
750	100	0.107	1.86
1000	75	0.112	1.95
1250	51	-	-
1500	32	0.093	1.63
1750	30	-	-
2000	15	0.086	1.51
2500	13	0.089	1.56
3000	10	0.091	1.58
4000	-	0.085	1.48
5000	-	0.076	1.33

y-intercept = 1.94×10^{-4}

slope = -1.32×10^{-8}

$r^2 = 0.82$

Table VIII
Data from Trial 2

# Shots	Laser Beam Energy (mj)	$A - A_o$	Concentration ($x10^{-4}$ M)
0	241	0.118	2.04
100	204	0.109	1.89
250	150	0.116	2.02
500	114	0.106	1.85
750	76	0.112	1.94
1000	48	0.113	1.96
1250	37	-	-
1500	27	0.100	1.74
1750	21	-	-
2000	13	0.100	1.74
2500	7	0.102	1.77
3000	4	0.106	1.85
4000	-	0.093	1.63
5000	-	0.091	1.58

y-intercept = 1.97×10^{-4}

slope = -7.77×10^{-9}

$r^2 = 0.75$

Table IX
Data from Trial 3

# Shots	Laser Beam Energy (mj)	$A - A_o$	Concentration ($x10^{-4}$ M)
0	211	0.115	1.99
100	169	0.114	1.98
250	126	0.117	2.02
500	88	0.115	1.99
750	58	0.112	1.95
1000	39	0.113	1.96
1250	30	-	-
1500	19	0.109	1.90
1750	18	-	-
2000	13	0.100	1.74
2500	7	0.104	1.80
3000	3	0.104	1.81
4000	-	0.099	1.73
5000	-	0.096	1.68

y-intercept = 2.00×10^{-4}

slope = -6.99×10^{-9}

$r^2 = 0.87$

Table X
Data from Trial 4

# Shots	Laser Beam Energy (mj)	$A - A_o$	Concentration ($x10^{-4}$ M)
0	224	0.111	1.92
100	184	0.110	1.91
250	221	0.110	1.91
500	195	0.114	1.98
750	213	0.118	2.04
1000	203	-	-
1250	184	-	-
1500	183	0.113	1.96
1750	171	-	-
2000	181	0.103	1.79
2250	158	-	-
2500	143	0.116	2.02
2750	114	-	-
3000	122	0.112	1.94

y-intercept = 1.94×10^{-4}

slope = -1.08×10^{-10}

$r^2 = 0$

Table XI
Data from Trial 5

# Shots	Laser Beam Energy (mj)	$A - A_o$	Concentration ($x10^{-4}$ M)
0	189	0.117	2.03
100	156	0.104	1.80
250	141	0.113	1.96
500	110	0.119	2.06
750	102	0.115	2.00
1000	75	0.111	1.93
1250	56	-	-
1500	42	0.113	1.96
1750	43	-	-
2000	35	0.120	2.07
2500	31	0.114	1.97
3000	31	0.116	2.01
3500	14	-	-
4000	10	0.106	1.85
4500	7	-	-
5000	8	0.101	1.76

y-intercept = 2.00×10^{-4}

slope = -2.84×10^{-9}

$r^2 = 0.21$

Table XII
Data from Trial 6

# Shots	Laser Beam Energy (mj)	$A - A_o$	Concentration ($x10^{-4}$ M)
0	88	0.114	1.98
100	97	0.115	1.99
250	86	0.107	1.85
500	84	0.114	1.98
750	87	0.106	1.85
1000	82	0.103	1.79
1250	78	-	-
1500	81	0.113	1.96
1750	81	-	-
2000	77	0.109	1.90
2500	69	0.117	2.03
3000	78	0.117	2.03
4000	-	0.108	1.88

y-intercept = 1.92×10^{-4}

slope = 7.37×10^{-10}

$r^2 = 0.01$

Appendix D

Determination of Oxygen Concentration in Solution

Determination of Oxygen Concentration in Solution

For absolute ethanol (99.7 percent) the Bunsen absorption coefficient α is defined by the equation

$$\alpha = 0.23370 - 0.00074688\ T_s + 0.000003288\ T_s^2 \qquad (20)$$

where T_s is the temperature (C). For $T_s = 20$ C, $\alpha = 0.22$.

Henry's law constant K_H and the Bunsen absorption coefficient are linked by

$$K_H = \frac{17{,}032{,}400\ (1 + b)}{M_W\ \alpha} \qquad (21)$$

where

$$b = \frac{M_W\ P_{O_2}\ \alpha}{17{,}032{,}400\ D} \qquad (22)$$

and

D = density of solvent

P_{O_2} = partial pressure of oxygen (mm Hg)

M_W = molecular weight of solvent

For ethanol at 20 C,

$$D = 0.78934 \text{ g/ml} \qquad (23)$$

$$M_W = 46.07 \text{ g/g-mole} \qquad (24)$$

For a 10.3 percent O_2 cover gas Eqs (21) and (22) can now be solved to give

$$b = 5.9 \times 10^{-5} \tag{25}$$

$$K_H = 1.3 \times 10^{6} \tag{26}$$

From Henry's law

$$x_{O_2} = \frac{P_{O_2}}{K_H} = 5.9 \times 10^{-5} \tag{27}$$

where x_{O_2} is the mole fraction of oxygen in solution. The concentration of ethanol is found by dividing the density by the molecular weight to give

$$[EtOH] = 17.1 \text{ g-mole/liter} \tag{28}$$

But

$$x_{O_2} = \frac{[O_2]}{\text{Total Concentration}} \cong \frac{[O_2]}{[EtOH]} \tag{29}$$

Therefore

$$[O_2]_{.103} = x_{O_2} [EtOH] = 1.0 \times 10^{-3} \text{ mole/liter} \tag{30}$$

For 21 percent O_2, the same sequence of calculations yields

$$[O_2]_{.21} = 2.1 \times 10^{-3} \text{ mole/liter} \tag{31}$$

(Ref 33:254-255)

VITA

John Michael Rabins was born 19 May 1951 in Los Angeles, California. He graduated from Mark Keppel High School in 1969 and attended the United States Air Force Academy, where he majored in Physics. In 1973 he was awarded a Bachelor of Science degree and was commissioned a Second Lieutenant in the United States Air Force. He was assigned as an Avionics Maintenance Officer at McChord AFB, Washington until June, 1977, when he entered the School of Engineering at the Air Force Institute of Technology.

Permanent address: 992 Kempton Avenue
Monterey Park, California 91754

UNCLASSIFIED

SECURITY CLASSIFICATION OF THIS PAGE (When Data Entered)

REPORT DOCUMENTATION PAGE		READ INSTRUCTIONS BEFORE COMPLETING FORM
1. REPORT NUMBER AFIT/GEP/AA/78D-1	2. GOVT ACCESSION NO.	3. RECIPIENT'S CATALOG NUMBER
4. TITLE (and Subtitle) STUDY OF THE CORRELATION BETWEEN DEGRADATION OF KITON RED S LASER DYE AND DEGRADATION OF LASER ENERGY UNDER FLASH CONDITIONS		5. TYPE OF REPORT & PERIOD COVERED MS Thesis 6. PERFORMING ORG. REPORT NUMBER
7. AUTHOR(s) John M. Rabins Captain USAF		8. CONTRACT OR GRANT NUMBER(s)
9. PERFORMING ORGANIZATION NAME AND ADDRESS Air Force Institute of Technology (AFIT-EN) Wright-Patterson AFB, Ohio 45433		10. PROGRAM ELEMENT, PROJECT, TASK AREA & WORK UNIT NUMBERS Project 2001 01 54
11. CONTROLLING OFFICE NAME AND ADDRESS Electro-Optic Sources Group (AFAL-DHO) Air Force Avionics Laboratory Wright-Patterson AFB, Ohio 45433		12. REPORT DATE December, 1978 13. NUMBER OF PAGES 90
14. MONITORING AGENCY NAME & ADDRESS(if different from Controlling Office)		15. SECURITY CLASS. (of this report) Unclassified 15a. DECLASSIFICATION DOWNGRADING SCHEDULE

16. DISTRIBUTION STATEMENT (of this Report)

Approved for public release; distribution unlimited

17. DISTRIBUTION STATEMENT (of the abstract entered in Block 20, if different from Report)

18. SUPPLEMENTARY NOTES

Approved for public release; IAW AFR 190-17

JOSEPH P. HIPPS, Major, USAF
Director of Information

19. KEY WORDS (Continue on reverse side if necessary and identify by block number)

Dye
Dye Laser
Photodegradation
Reaction Kinetics

20. ABSTRACT (Continue on reverse side if necessary and identify by block number)

The laser dye Kiton Red S dissolved in ethanol was degraded under flashlamp excitation in a dye laser. Data obtained with infrared spectral analysis were used to construct plots of dye concentration versus shot number. From these plots the degradation reaction was found to be zeroth order in Kiton Red S. A rate equation was determined. Laser energy was monitored in order to allow for a comparison between laser degradation and dye degradation. The effect of both different oxygen concentrations and different excitation wavelengths on the reaction rate was observed. Based upon the experimental results a reaction mech-

DD FORM 1 JAN 73 1473 EDITION OF 1 NOV 65 IS OBSOLETE

UNCLASSIFIED

SECURITY CLASSIFICATION OF THIS PAGE (When Data Entered)

anism was proposed. Two photoreaction products were postulated, one which absorbs laser radiation, and another which is reactive with the triplet dye molecules.